

# Computation-friendly Graph Neural Network Design by Accumulating Knowledge on Large Language Models

Jialiang Wang<sup>1</sup>, Shimin Di<sup>1</sup>, Hanmo Liu<sup>2</sup>, Zhili Wang<sup>1</sup>, Jiachuan Wang<sup>1</sup>, Lei Chen<sup>2,1</sup>, Xiaofang Zhou<sup>1</sup>

<sup>1</sup>The Hong Kong University of Science and Technology, Hong Kong SAR, China

<sup>2</sup>The Hong Kong University of Science and Technology (Guangzhou), Guangzhou, China

{jwangic,sdiaa,hliubm,zwangeo,jwangey}@connect.ust.hk,{leichen,zxf}@cse.ust.hk

## ABSTRACT

Graph Neural Networks (GNNs), like other neural networks, have shown remarkable success but are hampered by the complexity of their architecture designs, which heavily depend on specific data and tasks. Traditionally, designing proper architectures involves trial and error, which requires intensive manual effort to optimize various components. To reduce human workload, researchers try to develop automated algorithms to design GNNs. However, both experts and automated algorithms suffer from two major issues in designing GNNs: 1) the substantial computational resources expended in repeatedly trying candidate GNN architectures until a feasible design is achieved, and 2) the intricate and prolonged processes required for humans or algorithms to accumulate knowledge of the interrelationship between graphs, GNNs, and performance.

To further enhance the automation of GNN architecture design, we propose a computation-friendly way to empower Large Language Models (LLMs) with specialized knowledge in designing GNNs, thereby drastically shortening the computational overhead and development cycle of designing GNN architectures. Our framework begins by establishing a knowledge retrieval pipeline that comprehends the intercorrelations between graphs, GNNs, and performance. This pipeline converts past model design experiences into structured knowledge for LLM reference, allowing it to quickly suggest initial model proposals. Subsequently, we introduce a knowledge-driven search strategy that emulates the exploration-exploitation process of human experts, enabling quick refinement of initial proposals within a promising scope. Extensive experiments demonstrate that our framework can efficiently deliver promising (e.g., Top-5.77%) initial model proposals for unseen datasets within seconds and without any prior training and achieve outstanding search performance in a few iterations.

## KEYWORDS

Graph Neural Networks, Neural Architecture Search, Large Language Models, Graph to Language

## 1 INTRODUCTION

Graph Neural Networks (GNNs) have solidified their role as state-of-the-art encoders in the realm of graph representation learning [31, 67, 75], effectively modeling complex real-world systems depicted as graphs [14, 23, 29, 44]. These networks operate on a message-passing schema, iteratively refining node representations through aggregate neighboring messages [9, 22, 54]. Designing an optimal GNN architecture for specific data and tasks, however, remains a formidable challenge. This process is not only time-consuming but also requires deep expertise [16]. Specifically, human experts often engage in labor-intensive trial and error, experimenting with

various network aggregation methods, inter-layer connections, and intra-layer configurations to identify effective solutions.

In response to this challenge, various automated algorithms [32, 41, 81] have been proposed to reduce the manual effort required in designing GNN architectures. Notably, Automated Graph Neural Networks (AutoGNNs) [16, 58, 80], a specialized branch of Automated Machine Learning (AutoML) [24], have been developed to search for optimal GNN configurations for given graphs and their associated tasks. Past research has demonstrated that AutoGNNs can significantly alleviate manual effort and enhance model performance [60, 61, 64]. Recently, the advent of Large Language Models (LLMs) [4, 10, 53] has inspired new avenue [52] that leverage LLMs to further replace some human involvement beyond the traditional capabilities of AutoGNNs, such as task understanding [12, 56] and problem formulation [62]. These LLM-based methods have demonstrated notable strides toward democratizing complex processes of designing GNN architectures. However, automated approaches, much like their human counterparts, continue to face two major issues: 1) the substantial computational resources expended in repeatedly trying candidate GNN architectures until a feasible design is achieved, and 2) the intricate and prolonged processes required for humans or algorithms to accumulate knowledge of the interrelationship between graph datasets, GNNs, and performance.

When human experts design GNNs, the process typically involves fully training each candidate architecture until convergence to evaluate its performance, followed by iterative refinements based on the feedback obtained. This cycle repeats numerous times until a high-performing model is developed. Though freeing human hands, current AutoGNNs still fundamentally rely on trying out different configurations and performing iterative optimizations, albeit with some efficiency enhancements such as weight sharing [13, 39] and learning curve prediction [1, 11]. Later, LLM-based approaches like GPT4GNAS [56] and Auto2Graph [62] have advanced the field by introducing more interpretable search strategies and user-friendly system configurations. However, these improvements have only modestly reduced the substantial computational resources and time required to design and deploy effective GNN architectures.

Moving beyond computational efficiency, human experts and automated algorithms all encounter significant challenges in *proficiency* [36, 58] (i.e., the ability to accumulate the knowledge of designing models), which critically hinges on their ability to accumulate, discern, and effectively apply intricate knowledge about the interrelationships between data characteristics, model architectures, and performance outcomes. Humans, akin to training a new Ph.D. student, face substantial hurdles in accumulating this complex knowledge, often undergoing a lengthy and iterative learning process to *proficiently* design effective GNN models. Similarly,

AutoGNNs conduct model searches specific to the data and task at hand but overlook the relationships between different datasets and models. As a result, these approaches require starting from scratch with each new dataset, thereby lacking *proficiency*. Moving forward, LLMs have shown potential in mimicking human-like knowledge accumulation in GNN architecture design [52]. However, current LLM-based approaches [12, 56, 62] confront three *non-proficiencies*. First, an inadequate understanding of graph data can lead to improper knowledge associations, undermining the effectiveness of model suggestions. This issue is exacerbated by an overreliance on simplistic, user-provided semantic descriptions of datasets, which overlook critical graph topology and lead to skewed interpretations of model preferences. Secondly, the native LLMs lack the nuanced knowledge necessary to establish a concrete and empirical mapping from datasets’ characteristics to effective model configurations. This deficiency results in overly generalized, poor-quality model suggestions for new datasets. Thirdly, the initial model proposals generated by LLMs are often superficial and require further refinement to ensure effectiveness. Unfortunately, current LLM-based methods primarily mimic simplistic search strategies, focusing merely on gathering superficial insights from the optimization trajectory [69]. In summary, while humans require a prolonged process to accumulate the knowledge necessary to become experts, current automated algorithms have weak abilities to become *proficient*.

In this paper, to promote the *proficiency* and reduce the associated high computational overhead in designing GNN architectures, we propose a computation-friendly way to design GNNs by accumulating knowledge on LLMs (abbreviate to DesiGNN). In this paper, to promote the *proficiency* and reduce the associated high computational overhead in designing GNN architectures, we propose a computation-friendly way to design GNNs by accumulating knowledge on LLMs (abbreviate to DesiGNN). To enable automated algorithms to become *proficient* like human experts, we focus on promoting LLM’s capability to capture the interrelationships between graphs, models, and performance. To achieve this goal and tackle the three non-proficiencies, we first propose to understand the correlation across different graph datasets, then establish a knowledge retrieval system to assess dataset similarities and extract configuration-level insights, so that LLMs can suggest initial model proposals with high *proficiency* in a short time. To improve the performance of initial model proposals, i.e., further exploring fine-grained architecture like AutoGNNs, we rapidly refine initial model proposals based on actionable intelligence derived from configuration-level insights, significantly accelerating the development cycle of feasible models. Our contributions are listed as:

- We propose a novel idea to empower LLM with specialized, nuanced knowledge for designing GNN architectures. This approach not only enables LLM to accumulate knowledge and suggest models like human experts but also enables it to explore fine-grained GNN architectures like past AutoGNN methods.
- To empower architecture designs with accumulated knowledge, DesiGNN establishes novel Graph Understanding and Knowledge Retrieval modules to distill tailored model configuration knowledge from the relaxed mappings between datasets and top-performing models. Therefore, DesiGNN can efficiently deliver a promising model proposal for an unseen graph within seconds.
- To further promote the performance of the designed GNN, DesiGNN proposes a new way to perform controlled and directional refinement upon the initial model proposal. It employs LLMs to swiftly identify and summarize potential patterns from transferred top-performing knowledge, rapidly exploring fine-grained GNN architectures in a few iterations.
- Through extensive testing across 11 graphs, DesiGNN reliably delivers Top-5.77% GNN architectures within seconds and without prior training. They can further be effectively refined within just a few iterations. DesiGNN substantially reduces the overall computational overhead and enhances short-run effectiveness in deployment.

## 2 RELATED WORK

### 2.1 Graph Neural Networks

GNNs have been promising methods for representation learning on graph data  $G$ . Based on the message passing framework [17], GNNs iteratively update node representations  $\mathbf{H}_v$  of node  $v$  by aggregating messages from neighboring nodes. The intra-layer and inter-layer message-passing process can be formulated as:

$$\begin{aligned} \text{inter: } \mathbf{M}_v &\leftarrow \text{agg}(\text{msg}(\mathbf{H}_u, \mathbf{H}_v) | u \in N(v)), \mathbf{H}_v \leftarrow \text{upd}(\text{comb}(\mathbf{H}_v, \mathbf{M}_v)), \\ \text{intra: } \mathbf{H}_v &\leftarrow \text{fuse}(\mathbf{H}_v^0, \mathbf{H}_v^1, \dots, \mathbf{H}_v^K). \end{aligned}$$

Most GNNs [2, 9, 22, 35, 54, 67] are specific instances of these equations, differing mainly in their choice of functions like  $\text{agg}(\cdot)$ ,  $\text{comb}(\cdot)$ ,  $\text{upd}(\cdot)$ , and  $\text{fuse}(\cdot)$ . For example, GCN [31] uses  $\text{MEAN}(\cdot)$  for aggregation and  $\text{SUM}(\cdot)$  for combination. JK-Net [68] enhances inter-layer message passing by proposing various  $\text{fuse}(\cdot)$  functions, ranging from simple  $\text{MAX}(\cdot)$  to adaptive ones  $\text{LSTM}(\cdot)$ .

**2.1.1 Automated GNNs.** AutoGNNs [16, 58, 80] aim to automatically find an optimal GNN architecture  $\theta$  for an unseen graph  $G^u$  using a controller  $\pi$  parameterized by  $\alpha$ , where the architecture  $\theta$  with network weight  $\omega$  can achieve best performance  $\mathcal{H}$  on  $G^u$ :

$$\theta^*, \omega^* = \arg \max_{\theta, \omega} \mathbb{E}_{\theta \sim \pi_\alpha(\theta)} [\mathcal{H}(\theta, \omega; G^u)]. \quad (1)$$

In AutoGNNs, the search space is typically divided into intra-layer [15, 59, 60] and inter-layer [27, 59, 60, 63, 77] designs, focusing on the configuration of message passing and layer connectivity. The search algorithms employed include reinforcement learning [15], evolutionary algorithms [48], and differentiable search [27, 59, 59], each offering different strategies for exploring the search space and optimizing architecture selection.

However, as introduced in Sec. 1, classic AutoGNNs still face poor *proficiency* and extensive computational overhead issues [36, 58]. For the given graph  $G^u$ , classic works gradually optimize configurations  $\theta$  without leveraging any prior knowledge—highlighting a lack of *proficiency* (see Fig. 1). Besides, the optimization process of solving Eq. (1) needs a lot of candidate architecture sampling in  $\theta \sim \pi_\alpha(\theta)$ , thus demanding substantial computational resources.

**2.1.2 NAS Bench for Graph.** Unlike other NAS benchmarks [8], NAS-Bench-Graph [40] (details in the Appx. A.3) offers a comprehensive dataset space, including 9 node classification benchmark datasets. Its model space encompasses 9 types of GNN layers (micro space) and 9 configurations of directed acyclic graphs (macro space), cataloging the empirical performance of 26,206 unique GNN

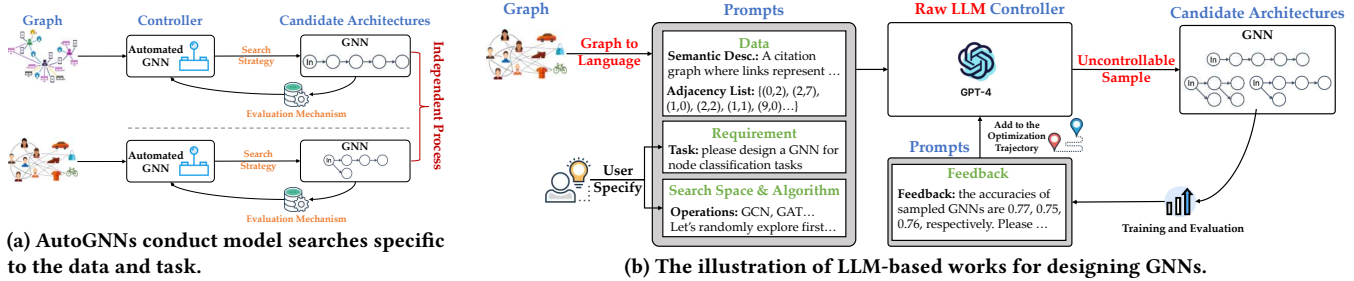


Figure 1: The illustration of how AutoGNNs and LLM-based works design GNN architectures.

architectures on each benchmark dataset. Therefore, the data-wise richness makes NAS-Bench-Graph an invaluable model configuration knowledge base, possessing the potential to reveal the intricate interrelationship between graphs, GNNs, and performance.

## 2.2 LLMs and Its Applications to GNNs

Recently, LLMs have shown remarkable *proficiency* in a variety of natural language understanding [47, 57] and task optimization scenarios [20, 69]. In this paper, we focus on the applications of LLMs to graphs and GNNs, especially designing GNNs by LLMs.

**2.2.1 LLMs with Graphs.** Recent advancements in integrating LLMs with graphs have significantly enhanced graph learning tasks [7, 42, 49] turning intricate graph details into more manageable formats for analysis and interpretation. In this integration, two primary lines of studies emerge. The first group involves using GNNs to process graph data into structured tokens, providing a solid foundation for LLMs to subsequently infer linguistic and contextual nuances [5, 50, 51]. Alternatively, LLMs may first enrich the raw graph data with contextual insights, which GNNs then utilize to refine their structural processing [43, 65, 66]. In the second group, deeper integration involves collaborative efforts such as fusion training [78] and alignment [33], where LLMs and GNNs synergistically enhance their functionalities to handle graph tasks more comprehensively. In a more autonomous approach, LLMs independently manage graph tasks, employing advanced language understanding to directly interpret and manipulate graph data [26, 55, 70]. This is exemplified by the “Graph to Language” (G2L) strategy [19], which utilizes LLMs to comprehend graph data through prompting.

Unfortunately, the research in this paper diverges from existing methods. To study the correlation between graphs, models, and performance, it not merely translates graphs into textual formats but also asks LLMs to assess and interpret graph similarities, which could directly reflect the preferences of different graph datasets for GNN architecture design. Specifically, it necessitates LLMs to prioritize understanding graph dataset characteristics and their implications on model performance, just like human expert intuitions.

**2.2.2 LLMs for Designing GNNs.** Recent research on the synergy between LLMs and AutoML, including GNN designs, has demonstrated a dynamic and powerful merger of language processing with structured data analysis and problem-solving [52]. These approaches differ primarily in how they acquire, condense, and utilize complex AutoML knowledge, thereby aiding LLMs in configuring [21, 74] and optimizing [28, 72, 76, 79] machine learning pipelines.

This reduces the necessity for complete retraining and diminishes the expertise required to effectively use AutoML.

As shown in Fig. 1b, recent explorations into integrating LLMs with GNN architecture design have opened new avenues for enhancing AutoGNN systems. Auto2Graph [62] utilizes LLMs to democratize the usage of traditional AutoGNNs, taking in semantic descriptions of datasets, task specifications, evaluation metrics, user preferences, and constraints to manage the complete lifecycle of graph learning tasks, from data processing to hyper-parameter tuning. GPT4GNAS [56] instead leverages GPT-4 to significantly reduce manual efforts in designing GNNs for new tasks by iteratively generating modular GNN architectures through carefully designed prompts that describe the search task, space, and strategy. GHGNAS [12] extends GPT4GNAS by incorporating simple descriptions of heterogeneous graphs, including node and edge types and numbers, to iteratively refine and enhance heterogeneous GNN designs.

Unfortunately, as shown in Fig. 1b, these approaches present notable limitations that our research seeks to address: 1) improper graph understanding, 2) lack of knowledge in raw LLMs, and 3) ineffective optimization strategies. First, current approaches [12, 56, 62] heavily rely on the quality and specificity of the user-provided descriptions, which can skew their effectiveness if the semantic description of the dataset is not correlated to the task. Moreover, they often overly trust the inherent reasoning ability of raw LLMs and do not account for any concrete knowledge between graph dataset and GNN performance, thus lacking the *proficiency*. Lastly, they rely on the optimization trajectory as the sole driving force for model refinement due to a lack of nuanced, actionable knowledge, limiting their effectiveness and computational efficiency in model refinement. As a result, they still require computationally intensive iterative exploration over the long run and have no control over the exploitation step, which is methodologically less *proficient* than how human experts refine GNN designs.

## 3 METHODOLOGY

As introduced in Sec. 1, the design of GNNs by both human experts and automated algorithms faces significant challenges including substantial computational resources and a lack of *proficiency*. To address these issues, we propose a computation-friendly way to design GNNs by accumulating knowledge on LLMs (DesiGNN). By comparing Fig. 1b and 2, DesiGNN is composed of three major different components, each designed to capture and leverage the intricate relationships between graphs, GNN configurations, and performance. Initially, the Graph Understanding module aims to automatically analyze graphs and identify the graph topology

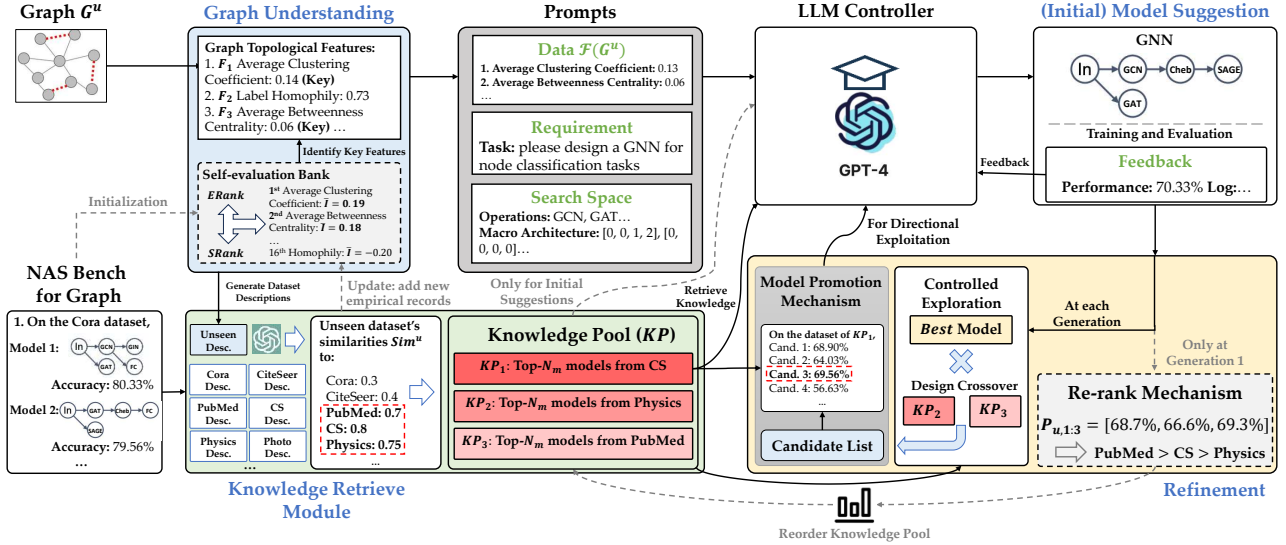


**Figure 2: The illustration of our DesiGNN pipeline for designing GNNs. The gray dash represents the initial operation (run once).**

that is crucial for enabling LLMs to assess the similarity between benchmark (within our knowledge) and unseen graph datasets (beyond our knowledge) with respect to model preference. Then, the Knowledge Retrieve module builds specialized model configuration knowledge from NAS-Bench-Graph [40], so that LLMs can utilize the insights gained from understanding graphs and retrieve relevant models as knowledge for unseen graphs. Lastly, the Model Suggestion and Refinement module leverages the retrieved knowledge to quickly suggest and refine the GNN proposals. In the subsequent sections, we explain how each component collectively contributes to a *proficient* and computationally efficient GNN design process.

### 3.1 Graph Understanding Module

To effectively accumulate tailored knowledge for specific datasets, it is crucial to first understand the characteristics and structures of the graphs. However, it remains an open problem to enable LLMs to understand the similarities between different graphs. Despite some progress in LLMs for graphs (see Sec. 2.2.1), existing works focus more on enabling LLMs to understand structured graph data given structured input (e.g., adjacent list), rather than the similarity among graphs. As discussed in Sec. 2.2.2, existing LLM-based approaches rely solely on user-provided semantic descriptions of datasets to initiate the process, while ignoring graph topology (or other characteristics). Besides, it is even more challenge to enable LLMs to capture the connection between graph similarity with GNN configuration (or GNN performance).

#### 3.1.1 Understand Graph Similarity and Motivational Experiments.

As discussed in previous works (see Sec. 2.2), the semantic description of graph data may be biased. Thus, to achieve the goal of building knowledge about “graph-GNN-performance”, we start with 16 graph topological features  $F = \{F_k\}_{k=1}^{16}$  (e.g., average shortest path length, details in Appx. A.2.1) to understand graph similarity from two aspects: 1) the similarity among graphs, and 2) the impact of graph similarity on the empirical performance of GNNs.

Given two graphs  $G^i$  and  $G^j \in G$ , let  $s_{ik}$  and  $s_{jk}$  denotes the statistical value of feature  $F_k$  on graphs  $G^i$  and  $G^j$ , respectively. Then, the distance  $Dist_k^{ij} = \sqrt{(s_{ik} - s_{jk})^2}$  computes the difference of feature  $F_k$  between  $G^i$  and  $G^j$ , i.e., negative  $\{Dist_k^{ij}\}_{k=1}^{16}$  can assess the topological similarities between graphs  $G^i$  and  $G^j$ . Then, to capture the difference in model performance, we let  $P^{ij}$  denote the performance of transferring model configuration knowledge gathered from another graph  $G^j$  to  $G^i$  (see Sec. 3.3.1). In other words, different from  $Dist_k^{ij}$  that evaluates the topological distance between graphs,  $P^{ij}$  tries to assess the similarity between graphs based on the effectiveness of knowledge transfer (empirical performance). Based on  $Dist_k^{ij}$  and  $P^{ij}$ , we formally define the statistical ranking  $SRank(i, k)$  and empirical ranking  $ERank(i)$  as follows:

$$SRank(i, k) = \text{argsort}(\{Dist_k^{ij} \mid j \neq i, G^j \in G\}, \text{ascending}), \quad (2)$$

$$ERank(i) = \text{argsort}(\{P^{ij} \mid j \neq i, G^j \in G\}, \text{descending}), \quad (3)$$

where  $SRank(i, k)$  represents the statistical similarity ranking of other graphs  $\{G^j \mid j \neq i, G^j \in G\}$  to graph  $G^i$  based on feature  $F_k$ , and  $ERank(i)$  represents the empirical similarity ranking of other graphs to graph  $G^i$ . Finally, to capture the impact of graph similarity (in terms of feature  $F_k$ ) on the empirical effectiveness of suggesting GNNs, we calculate the Kendall Rank Correlation Coefficient [30] between  $SRank(i, k)$  and  $ERank(i)$  as follows:

$$I(G^i, F_k) := \text{KendallCorr}(SRank(i, k), ERank(i)), \quad (4)$$

where  $I(G^i, F_k)$  evaluates the correlation between the statistical differences in feature  $F_k$  (between  $G^i$  and other graphs  $\{G^j\}$ ) and the empirical differences in transferring knowledge from other graphs  $\{G^j\}$  to  $G^i$ . In other words,  $I(G^i, F_k)$  can be the “confidence” of graph topological feature  $F_k$  to determine the empirical similarity between  $G^i$  and other graph data within our knowledge. That is, the larger  $I(G^i, F_k)$  is, the more  $F_k$  is a strong correlation indicator on  $G^i$  that can determine whether other graphs  $\{G^j\}$  is related to  $G^i$  from the perspective of graph topology and empirical performance.

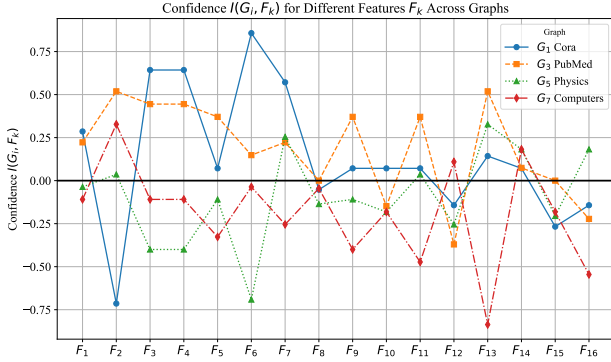


**Figure 3: A depiction of the feature confidences across different datasets.**

As introduced in Sec. 2.1.2, NAS-Bench-Graph [40] contains 9 benchmark graphs and 26,206 unique GNN architectures. Thus, we first study the correlation  $I(G^i, F_k)$  between graph topological features and the empirical performance of GNNs on the benchmark datasets. For each anchor graph  $G^i$ , we compare it with the other 8 graphs and calculate the correlation  $\{I(G^i, F_k)\}_{k=1}^{16}$ , i.e., 16 feature confidences on  $G^i$ . As shown in Fig. 3,  $I(G^i, F_k)$  on different anchor graph fluctuates greatly, e.g.,  $I(\text{Physics}, \text{Label Homophily})$  is positive but others are negative. That is, some features can be used to judge whether two data are strongly associated (statistical and empirical evaluation) on one graph, but the feature may be unreliable on other graphs. In summary, not only are some semantic descriptions difficult to describe graph similarities, but even statistical and empirical indicators cannot be directly used as invariant indicators to characterize the correlation between graphs and the impact of these correlations on model performance.

**3.1.2 Adaptive Filtering Mechanism.** As summarized in Sec. 3.1.1, even statistical and empirical indicators cannot be directly used as invariant indicators to characterize the correlation between graphs and the impact of these correlations on model performance. Thus, we propose an adaptive filtering mechanism to identify the most influential set of graph topological features, bridging the gap between the graph dataset and GNN designs with performance-driven data understanding. We treat each benchmark graph as an anchor  $G^i$  in turn, compute the  $I(G^i, F_k)$  for each  $F_k$ , and average them on all  $n$  benchmark graphs to obtain the average correlation coefficient:  $\bar{I}(F_k) = \frac{1}{n} \sum_{i=1}^n I(G^i, F_k)$ , where  $\bar{I}(F_k)$  is calculated based on the records in NAS-Bench-Graph [40]. Then, the filter  $\mathcal{F}(G^i)$ , initiated using benchmark data within seconds, selects the Top- $N_f$  average correlation coefficients  $\{\bar{I}(F_k)\}$  as the most influential sets of graph topological features. Thus, it circumvents “artificial hallucinations” often triggered by unprofessional or misleading user input. Additionally, we design a self-evaluation bank  $BE$  that stores the measured graph topological features and the empirical similarity rankings of new datasets throughout our lifecycle, ensuring the filter  $\mathcal{F}(G^i)$  is continuously updated (i.e., adaptive filter). By grounding feature selection on the empirical performances of initial model proposals, this mechanism sets a stage for capturing the graph-to-graph ( $G^i$  to  $G^j$ ) relationship that can reveal correlations from graphs to top-performing GNN models  $\mathcal{M} : (G, \theta) \rightsquigarrow P$ .

## 3.2 Knowledge Retrieval Module

The *proficiency* of the GNN architecture design process critically depends on the ability to accumulate, discern, and effectively apply intricate knowledge about the interrelationships between graphs, GNNs, and performance as  $\mathcal{M} : (G, \theta) \rightsquigarrow P$ . However, as illustrated in Fig. 1, AutoGNNs often lack this data-wise knowledge prior to extensive training, while native LLMs only have limited capabilities to design some more general GNNs as studied in Appx. B.3.1. To bridge this gap, we utilize the detailed records of model-to-performance relationships captured in NAS-Bench-Graph [40], which contains diverse and intricate mappings across various graphs, a wide range of candidate GNNs, and their corresponding performance.

To capture the complex “Graph-GNN-Performance” correlations, we encapsulate the Top- $N_m$  model designs from NAS-Bench-Graph [40] to serve as concrete summaries of model preferences for different benchmark graphs. Further, we associate these model summaries with their corresponding filtered features generated by the Graph Understanding module of Sec. 3.1 (i.e., using natural language to describe graph topological features and GNN models), then creating 9 distinct knowledge bases for selective retrieval. This strategy simplifies the complex interrelationships into more manageable correlations between datasets and their top-performing models:  $\mathcal{M}^* : G \rightarrow \theta^*$ . Then, we employ LLMs to analyze and compare the similarities between an unseen dataset  $G^u$  (user inputs) and benchmark graphs  $G = \{G^i\}_{i=1}^9$  (within our knowledge) as follows:

$$\text{Sim}^u = \{\mathcal{L}\mathcal{L}\mathcal{M}_{\text{GDC}}(\mathcal{F}(G^u), \mathcal{F}(G^i))\}_{i=1}^9, \quad (5)$$

where we transform the filtered features  $\mathcal{F}(\cdot)$  into natural language before feeding them into GPT-4  $\mathcal{L}\mathcal{L}\mathcal{M}_{\text{GDC}}(\cdot, \cdot)$ . As shown in Fig. 2, this process is conceptualized as a prompt design problem, where  $\mathcal{L}\mathcal{L}\mathcal{M}_{\text{GDC}}(\cdot, \cdot)$  is tasked with analyzing the descriptions of both unseen and benchmark graphs. The objective is to generate task similarities that correlate with the top-performing model patterns. This method effectively leverages the complex mappings captured in NAS-Bench-Graph [40] and adapts to the variability across graphs, thereby facilitating the retrieval of specialized, most relevant model configuration knowledge from the benchmark graph to the unseen.

To retrieve the most relevant knowledge to unseen graph  $G^u$ , we rank benchmark graphs based on their similarities  $\text{Sim}^u$  and select Top- $N_s$  most similar graphs. Then, the Knowledge Pool  $KP$  for  $G^u$  is formed by collecting the top-performing models  $\{\theta_{im}^*\}_{m=1}^{N_m}$  from each one of selected Top- $N_s$  benchmark graphs  $G^i$ , defined as:

$$KP = \bigcup_{G^i \in \text{Top-}N_s(\text{Sim}^u)} \{(G^i, \{\theta_{im}^*\}_{m=1}^{N_m})\}, \quad (6)$$

where  $KP_i = \{(G^i, \{\theta_{im}^*\}_{m=1}^{N_m})\}$  and  $G^i$  is the  $i$ -th graph similar to  $G^u$ . This retrieval strategy collects the Top- $N_m$  model designs from each similar benchmark graph for in-context learning. It streamlines the transfer of GNN configuration knowledge to  $G^u$  and leverages the analytical capabilities of LLMs to ensure an effective, efficient, and interpretable knowledge accumulation process.

## 3.3 GNN Model Suggestion and Refinement

**3.3.1 Initial Model Suggestion.** As shown in Fig. 2, after understanding the graphs in Sec. 3.1 and building knowledge in Sec. 3.2, the LLM acts as a surrogate agent to facilitate the initial model

suggestion process. This step integrates user requirements with the top model designs from each of the retrieved knowledge bases in  $KP$  and a detailed description of the search space, including the macro architecture and operation lists from NAS-Bench-Graph [40]. The initial model proposals are suggested by LLMs as follows:

$$\theta_{ui} \leftarrow \mathcal{LLM}_{IMS}(\mathcal{F}(G^u), KP_i), P^{ui} = \mathcal{H}(\theta_{ui}, \omega; G^u), \quad (7)$$

where  $\theta_{ui}$  is the  $i$ -th suggested model for the unseen graph  $G^u$  based on the knowledge pool  $KP_i$  of benchmark graph  $G^i$ , and  $P^{ui}$  is the training performance of  $\theta_{ui}$  on  $G^u$ . This process is designed to swiftly generate  $N_s$  initial model proposals for the unseen graph  $G^i$ , each leveraging specialized knowledge from different benchmark graphs. Then, our framework will undertake experimental validation to assess each model’s performance. Compared with AutoGNNs, this streamlined approach does not launch training before generating proposals. Thus, it not only significantly accelerates the model suggestion phase compared to classic AutoGNNs but also enhances the effectiveness of the models due to the integration of empirically derived configuration knowledge. Notably, our initial model suggestions can even surpass existing automated approaches that have iteratively refined 30 proposals (Appx. B.2.2).

**3.3.2 Model Proposal Refinement.** To further enhance the effectiveness of the initial model proposals, we propose a more structured, knowledge-driven refinement strategy. This refinement strategy enables LLMs to refine models in a nuanced and fine-grained manner, emulating the exploration-exploitation process of human experts. By incorporating specific, empirically derived configuration knowledge into the refinement phase, we ensure that each refinement step is clearly informed by a deep understanding of what configurations have historically led to success under similar circumstances.

As formalized in Algo. 1, the process begins with (1) **Re-rank Mechanism:** The knowledge bases in  $KP$  are re-ranked according to the performance ranking of the corresponding initial model proposals  $\{\theta_{ui}\}_{i=1}^{N_s}$ . The best proposal  $\theta_{u1}$  is chosen as the starting point. (2) **Controlled Exploration:** Configurations within  $KP_{2:N_s}$  are utilized to crossover the best proposal, yielding  $N_c$  candidates. (3) **Model Promotion Mechanism:** These candidates are ranked based on their retrieved performances on the benchmark dataset of  $KP_1$ , with the most promising candidate  $\theta_u^{t'}$  advanced for further refinement at iteration  $t$ . (4) **Directional Exploitation and Optimization:** A comprehensive prompt that includes user requirements, task descriptions, search space details, previous training logs, and the optimization trajectory  $\theta_u^T$  guides the LLM controller  $\text{LLM}_{GNAS}$  to mutate the promoted candidate  $\theta_u^{t'}$  using elite insights from  $KG_1$ . The refined model proposal  $\theta_u^t$  is automatically constructed and trained to evaluate its performance  $P_u^t$ . The results  $(\theta_u^t, P_u^t)$  are appended into the optimization trajectory  $\theta_u^T$ . If it surpasses the current best, it is updated as the new  $\theta_u^*$ .

## 4 EXPERIMENTS

### 4.1 Experimental Settings

**4.1.1 Task and Data Sets.** Our experiments are conducted under the benchmark setting defined in NAS-Bench-Graph [40], focusing on the node classification across 8 benchmark graphs (except for ogbn-proteins, see Appx. B.1.1): Cora [45], Citeseer [45], PubMed

[45], CS [46], Physics [46], Photo [46], Computer [46], and ogbn-arXiv [25]. Additionally, we include 3 graphs beyond benchmarks: DBLP [3], Flickr [73], and Actor [38]. Detailed statistics are in Tab. 4.

**4.1.2 Baselines.** We benchmark against a variety of models, spanning manually designed GNNs and automated designed algorithms. Seven manually designed GNNs [2, 9, 22, 31, 35, 54, 67] illustrate labor- and expertise-intensive GNN design without automation. The classic search strategies [18, 34], including Random [32], Evolutionary Algorithms (EA) [41], and Reinforcement Learning (RL) [81], search optimal GNN architectures from the same search space as our approach. Besides, GNAS [16], and Auto-GNN [80] are automated yet non-knowledge-driven design approaches. We also consider two posterior similarity-based methods to study the effectiveness of our graph understanding module. Kendall rank correlation coefficient [71] and overlapping ratio of the Top 5% architectures [40] will output the best model design from the most similar graph serve as the initial model proposals. For LLM-based methods, we reproduce GPT4GNAS [56] and GHGNAS [12] as no available code. Auto2Graph [62] calls GPT APIs to combine with AutoGNNs, while its underlying algorithms have been covered by our other baselines.

**4.1.3 Evaluation Measurement.** The outputs of automated algorithms (including AutoGNNs and LLM-based works) are sometimes affected by stochastic algorithms (e.g., Random, EA, RL) and unstable response time of GPT APIs. For a fair comparison, we report the average accuracy of designed GNNs across ten runs to ensure reliability. Besides, to assess short-run efficiency, we evaluate the best-so-far accuracy after different numbers of model proposals are validated by automated algorithms: 1-30 proposals in Fig. 4.

**4.1.4 Implementation Details.** DesiGNN is implemented using PyTorch [37] and LangChain (GPT-4) [6]. Detailed settings on the training and module hyperparameters are provided in Appx. B.1.2 and B.1.3, respectively. We use `DesiGNN-Init` to denote the initial model proposals suggested by DesiGNN in Sec. 3.3.1, and `DesiGNN` to represent the whole framework with model refinement in Sec. 3.3.2.

Our experiments adopt the NAS-Bench-Graph [40] as the source of accumulated knowledge and the unified search space (Appx. A.3.2). To prevent data leakage and ensure the integrity of results on benchmark graphs, we anonymize their descriptions and remove corresponding knowledge sources during the knowledge retrieval when they are treated as unseen. i.e., for trials involving datasets in the benchmark, we treat one graph as unseen and the other 8 benchmark graphs as available knowledge. DBLP, Flickr, and Actor can still approach all 9 benchmark graphs as knowledge. This rigorous setup is further guaranteed by the case study in Appx. B.3.1, which verifies that the LLMs, given dataset description alone, lack prior knowledge about effective model architectures within the NAS-Bench-Graph [40] search space. Besides, the unified search space ensures that all baselines are assessed under uniform conditions.

### 4.2 Main Results

**4.2.1 Initial Model Suggestions.** As shown in Tab. 1, we first examine the effectiveness of our initial model suggestions `DesiGNN-Init`. Traditional models like GCN and GAT excel on popular datasets such as Cora, Citeseer, and PubMed, but they fall short on less common datasets like Flickr and Actor. Instead, `DesiGNN` outperforms

**Table 1: The initial performance comparison (accuracy with standard derivation) of GNN designed by different works. Note that  $N_s = 3$  for DesiGNN-Init. We mark the best performance in bold, and underline best in manual and automated baselines.**

Type	Model	Cora	Citeseer	PubMed	CS	Physics	Photo	Computer	arXiv	DBLP	Flickr	Actor
<b>Manual</b>	GCN [31]	80.97(0.39)	69.90(1.26)	77.46(0.61)	88.65(0.57)	90.85(1.20)	89.44(0.48)	83.16(0.55)	71.08(0.16)	84.25(0.25)	54.27(0.14)	24.78(1.79)
	GAT [54]	80.83(0.47)	<u>70.70(0.71)</u>	75.93(0.26)	88.72(0.73)	89.47(1.14)	<u>89.93(1.75)</u>	<u>81.35(1.26)</u>	<u>71.24(0.10)</u>	84.98(0.15)	51.85(0.26)	26.91(1.09)
	SAGE [22]	79.47(0.31)	66.13(0.90)	75.50(1.14)	87.81(0.18)	<u>91.43(0.29)</u>	88.29(1.03)	81.46(0.73)	70.78(0.17)	<u>85.41(0.06)</u>	52.84(0.19)	30.13(0.70)
	GIN [67]	79.77(0.38)	63.30(1.26)	76.74(0.86)	81.08(3.09)	<u>86.67(0.86)</u>	87.37(1.01)	73.95(0.16)	61.33(0.70)	<u>82.82(0.82)</u>	51.08(0.08)	27.15(0.38)
	ChebNet [9]	79.40(0.57)	67.03(1.02)	75.13(0.49)	89.50(0.36)	89.75(0.87)	86.65(0.77)	79.10(2.26)	70.87(0.10)	84.84(0.21)	53.75(0.16)	30.46(0.77)
	ARMA [2]	78.33(0.69)	66.20(0.75)	75.00(0.51)	<u>89.87(0.35)</u>	88.88(1.09)	86.55(3.35)	78.47(0.57)	70.87(0.17)	84.31(0.30)	54.23(0.04)	31.29(0.43)
	k-GNN [35]	78.06(0.47)	30.97(3.56)	75.38(0.97)	83.81(0.58)	88.98(0.54)	86.45(0.21)	76.31(1.34)	63.18(0.38)	83.59(0.07)	51.18(0.33)	<u>32.74(0.68)</u>
<b>Simil.-based</b>	Kendall [71]	67.73	<u>69.20</u>	71.80	88.56	<u>91.56</u>	88.90	76.85	71.49	-	-	-
	Overlap [40]	<u>79.36</u>	<u>67.30</u>	71.80	88.56	89.95	<u>90.37</u>	76.85	<u>71.68</u>	-	-	-
<b>NNI [6]</b>	Random [32]	77.87(2.41)	66.64(1.32)	74.16(1.68)	81.78(9.41)	90.59(0.94)	89.04(2.55)	76.61(3.56)	68.93(1.82)	76.45(7.53)	52.50(0.72)	30.90(3.75)
	EA [41]	78.23(1.04)	66.40(2.63)	72.88(2.11)	87.03(2.64)	88.07(2.41)	87.30(1.38)	77.56(6.42)	68.28(2.95)	85.13(0.38)	53.22(0.92)	31.69(2.95)
	RL [81]	73.44(8.11)	65.35(2.40)	75.44(1.24)	86.17(5.09)	88.15(4.24)	89.48(1.35)	<u>77.70(3.07)</u>	68.00(4.71)	84.18(0.50)	52.07(2.84)	31.72(4.60)
<b>AutoGL [18]</b>	GNAS [16]	78.55(1.20)	63.25(5.87)	73.04(1.64)	86.04(7.88)	89.54(1.52)	87.27(2.96)	70.96(9.66)	69.94(1.71)	84.46(0.41)	<u>54.67(0.54)</u>	32.31(3.25)
	Auto-GNN [80]	78.58(2.18)	65.60(2.69)	<u>76.07(0.77)</u>	89.06(0.42)	89.26(1.51)	89.34(1.75)	77.49(3.41)	67.62(1.72)	84.67(0.62)	<u>50.97(1.21)</u>	30.18(4.67)
<b>LLMs</b>	GPT4GNAS [56]	78.50(0.37)	67.46(0.76)	73.89(0.86)	<u>89.26(0.38)</u>	89.44(1.94)	89.12(2.26)	77.21(5.26)	68.98(1.22)	84.93(0.22)	52.47(0.10)	34.26(0.47)
	GHGNAS [12]	79.13(0.45)	67.35(0.44)	74.90(0.57)	89.15(0.81)	88.94(2.57)	89.42(1.99)	77.04(3.96)	69.66(1.28)	85.06(0.15)	52.48(0.23)	33.72(2.72)
<b>Ours</b>	<b>DesiGNN-Init</b>	80.31(0.00)	69.20(0.16)	76.60(0.00)	89.64(0.08)	92.10(0.00)	91.19(0.00)	82.20(0.00)	71.50(0.00)	85.56(0.24)	55.16(0.11)	34.41(0.48)
	<b>DesiGNN</b>	<b>81.77(0.40)</b>	<b>71.00(0.09)</b>	<b>77.57(0.29)</b>	<b>90.51(0.42)</b>	<b>92.61(0.00)</b>	<b>92.38(0.06)</b>	<b>84.08(0.66)</b>	<b>72.02(0.18)</b>	<b>85.89(0.21)</b>	<b>55.44(0.06)</b>	<b>37.57(0.62)</b>

these GNNs that have been manually refined over the years. This observation suggests that conventional GNNs may be overly specialized, whereas DesiGNN offers a robust advantage in handling diverse graphs. Besides, DesiGNN-Init could surpass two posterior similarity-based methods, Kendall and Overlap, demonstrating the effectiveness of the graph understanding module in Sec. 3.1. Furthermore, compared with automated algorithms (NNI, AutoGL, and other LLM-based works), the first GNN proposed by DesiGNN-Init achieves competitive performance on 11 graph datasets. This highlights the superior performance of our knowledge-driven approach over classic automated methods, which lack such detailed insights, and LLM-based works, which rely only on generalized high-level knowledge. Specifically, we further conduct the case study to demonstrate that existing LLM-based works repeatedly suggest a few general GNN architectures as initial proposals, as detailed in Appx. B.3.1. This indicates that LLMs cannot provide the domain-specific designs for the unseen graph without extra knowledge. But on the other hand, DesiGNN can design different architectures for different graphs. In summary, through the comparison of results in Tab. 1, we can conclude that DesiGNN-Init with Graph Understanding (Sec. 3.1) and Knowledge Retrieval modules (Sec. 3.2) can give quite good initial model suggestions (Sec. 3.3.1), i.e., be more *proficient*.

**4.2.2 Model Refinement and Short-run Efficiency.** Compared with DesiGNN-Init, DesiGNN in Tab. 1 quickly optimizes the initial proposals in a few iterations (Sec. 3.3.2), thus surpassing all manually designed GNN competitors across 11 graphs. This validates the effectiveness of DesiGNN in designing GNNs by retrieving knowledge and performing refinement.

Automated algorithms need to verify multiple candidate GNN proposals. As the number of verified proposals increases, the searched frameworks generally become better. Thus, we assess the short-run

**Table 2: Computational resources (unit in proposal validations) needed by baselines to reach our 10-validations performance. \* means at least 1 over 10 trials failed to achieve within 100 validations (excluded from reported values).**

Model	#Model Proposal Validations										
	Cora	Cit.	Pub.	CS	Phy.	Pho.	Com.	arX.	DBL.	Fli.	Act.
<b>GNAS</b>	40.3*	48.3*	21.5*	38.8	>100*	66*	34.8	55*	69.4	77.2*	35.6
<b>Auto-</b>	21.8*	>100*	11.6	18.4	43*	29.3*	17*	59.3*	76.2*	>100*	15.6
<b>Rand.</b>	21.7*	>100*	45	18.8	89*	33*	22	87*	64.7	>100*	16.4
<b>EA</b>	24.7*	>100*	48.8*	40.8*	>100*	23*	51.3*	72.8*	>100*	46.3	14.8
<b>RL</b>	82*	>100*	11.8	14.8	>100*	84.5*	48.2	37*	38.8	99*	14
<b>GPT4G.</b>	30-40	>50	40-50	10	>50	30-40	10-20	40-50	40-50	>50	10-20
<b>GHGN.</b>	20-30	>50	40-50	10	>50	20-30	20-30	30-40	>50	>50	10

efficiency based on the number of proposals required to achieve the desired performance level, i.e., the fewer proposals to verify, the higher the efficiency. Fig. 4 (complete results in Appx. B.2.2) demonstrates that DesiGNN, which emulates the refinement strategies of human experts, generally achieves faster improvements in model performance, which is also verified in the ablation studies in Appx. C.1 and C.4. Besides, Tab. 2 shows that, to achieve the performance of DesiGNN after 10 proposal validations, the number of proposals required by other automated methods is far more than 10. This also further verifies that DesiGNN does not waste too many computing resources by repeatedly verifying and iterating candidate proposals. And it reinforces our claim of utilizing accumulated knowledge for immediate feedback and rapid optimization cycles.

### 4.3 Retrieve Knowledge with Graph Similarity

In Tab. 1, we show a preliminary comparison between DesiGNN-Init and other posterior similarity-based methods, showing that our

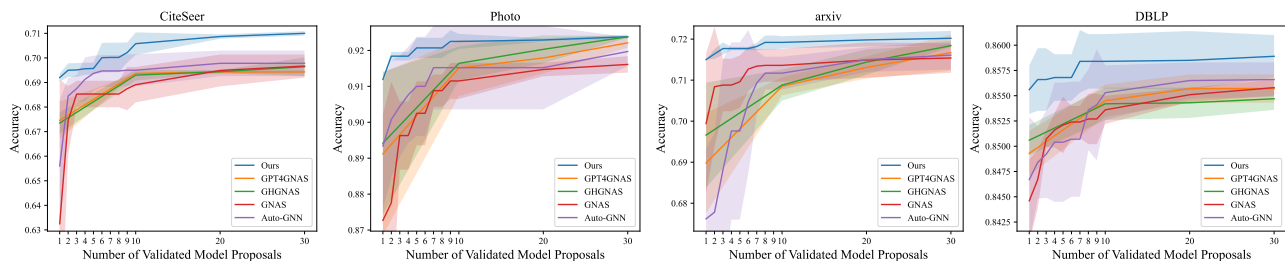


Figure 4: Short-run performance of empirically stronger automated baselines after validating 1-30 proposals.

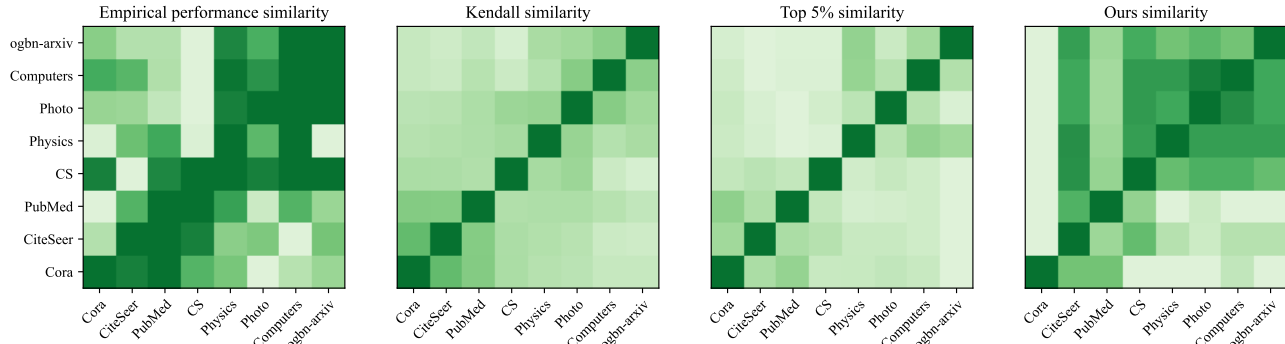


Figure 5: The similarities between datasets computed by empirical performance (target), Kendall rank correlation coefficient, and ours. The last figure shows the matching degree (to target) of the Top-3 similar datasets calculated by different methods.

initial model suggestion based on retrieving knowledge with similarity function Eq. (5) is empirically better than other baselines. In this subsection, we delve deeper into the pivotal design of our framework, retrieving knowledge of designing GNNs based on the graph similarity we proposed.

To demonstrate the effectiveness of our knowledge retrieval strategy, we evaluated whether our graph similarity could accurately identify the empirically most similar benchmarks, which is crucial as it empowers LLMs with the most relevant knowledge for suggesting high-performing initial model proposals on unseen datasets. For a more intuitive comparison, we plot the heatmap of similarities between benchmark graphs in Fig. 5. As we discussed before, the similarity between graph  $G^i$  and  $G^j$  is to determine the performance of knowledge transfer from  $G^j$  to  $G^i$ , i.e., empirical performance similarity  $P^{ij}$  in Fig. 5. However, we can see that Kendall similarity and Top 5% similarity are not as close to empirical similarity as our similarity, demonstrating that our training-free similarity measurer is competitive with posterior methods. Besides, more studies illustrating how semantic descriptions obstruct LLM’s ability to analyze data similarity are shown in Appx. B.3.2.

Additionally, we quantify the hit rate of different graph understanding and comparison settings in correctly identifying the empirically most relevant knowledge (i.e., can be used to recommend the best GNNs) in the available knowledge base within their  $N_s$  choices. As shown in Tab. 3, our dataset description with 8 most influential features and no semantic information, consistently achieves the highest hit rate across all settings. This validates that it is very important to select key graph topological features in Sec 3.1.2. It is noteworthy that relying solely on semantic descriptions or combining them with graph topological features results in a lower hit rate. Compared with directly using the key features to calculate

Table 3: Best benchmark hit rate (%) across unseen datasets.

Top-s Benchmarks	$N_s=1$	$N_s=2$	$N_s=3$
Statistical Similarity (w/o LLMs)	37.50	50.00	62.50
Semantic Only (LLMs)	26.25	50.00	57.50
Features Only (LLMs)	37.50	60.00	72.50
Both (LLMs)	27.50	50.00	60.00

statistical similarity, LLM’s reasoning ability enables it to adaptively balance the weights of different features, showing better results and flexibility in practice.

## 5 CONCLUSION

In this study, we propose a new framework DesiGNN for *proficiently* designing Graph Neural Networks (GNNs) using Large Language Models (LLMs). By first integrating topological graph understanding and then specialized knowledge retrieval, DesiGNN rapidly produces initial GNN models that are further refined efficiently to closely align with specific dataset characteristics and actionable prior knowledge. Experimental results demonstrate that DesiGNN expedites the design process by not only delivering top-tier GNN designs within seconds but also achieving outstanding search performance in a few iterations.

While effective within the graph domain, DesiGNN’s current application is limited by the available graph data, task, and model space defined in the open benchmark [40]. Future research could develop more nuanced mappings between more diverse datasets, more delicate configuration space, and the corresponding performance on other tasks, e.g., link prediction. Looking ahead, there are promising avenues for extending our knowledge-driven model design pipeline to broader machine learning contexts beyond graph data, e.g., image and tabular data.



## REFERENCES

- [1] Bowen Baker, Otkrist Gupta, Ramesh Raskar, and Nikhil Naik. 2017. Accelerating neural architecture search using performance prediction. *arXiv preprint arXiv:1705.10823* (2017).
- [2] Filippo Maria Bianchi, Daniele Grattarola, Lorenzo Livi, and Cesare Alippi. 2021. Graph neural networks with convolutional arma filters. *IEEE transactions on pattern analysis and machine intelligence* 44, 7 (2021), 3496–3507.
- [3] Aleksandar Bojchevski and Stephan Günnemann. 2017. Deep gaussian embedding of graphs: Unsupervised inductive learning via ranking. *arXiv preprint arXiv:1707.03815* (2017).
- [4] Tom Brown, Benjamin Mann, Nick Ryder, Melanie Subbiah, Jared D Kaplan, Prafulla Dhariwal, Arvind Neelakantan, Pranav Shyam, Girish Sastry, Amanda Askell, et al. 2020. Language models are few-shot learners. *Advances in neural information processing systems* 33 (2020), 1877–1901.
- [5] Ziwei Chai, Tianjie Zhang, Liang Wu, Kaiqiao Han, Xiaohai Hu, Xuanwen Huang, and Yang Yang. 2023. Graphllm: Boosting graph reasoning ability of large language model. *arXiv preprint arXiv:2310.05845* (2023).
- [6] Harrison Chase. 2022. *LangChain*. <https://github.com/langchain-ai/langchain>
- [7] Zhikai Chen, Haitao Mao, Hang Li, Wei Jin, Hongzhi Wen, Xiaochi Wei, Shuaiqiang Wang, Dawei Yin, Wenqi Fan, Hui Liu, et al. 2024. Exploring the potential of large language models (llms) in learning on graphs. *ACM SIGKDD Explorations Newsletter* 25, 2 (2024), 42–61.
- [8] Krishna Teja Chitty-Venkata, Murali Emami, Venkatram Vishwanath, and Arun K Somani. 2023. Neural architecture search benchmarks: Insights and survey. *IEEE Access* 11 (2023), 25217–25236.
- [9] Michaël Defferrard, Xavier Bresson, and Pierre Vandergheynst. 2016. Convolutional neural networks on graphs with fast localized spectral filtering. *Advances in neural information processing systems* 29 (2016).
- [10] Jacob Devlin, Ming-Wei Chang, Kenton Lee, and Kristina Toutanova. 2018. Bert: Pre-training of deep bidirectional transformers for language understanding. *arXiv preprint arXiv:1810.04805* (2018).
- [11] Tobias Domhan, Jost Tobias Springenberg, and Frank Hutter. 2015. Speeding up automatic hyperparameter optimization of deep neural networks by extrapolation of learning curves. In *Twenty-fourth international joint conference on artificial intelligence*.
- [12] Haoyuan Dong, Yang Gao, Haishuai Wang, Hong Yang, and Peng Zhang. 2023. Heterogeneous graph neural architecture search with gpt-4. *arXiv preprint arXiv:2312.08680* (2023).
- [13] Thomas Elsken, Jan-Hendrik Metzen, and Frank Hutter. 2017. Simple and efficient architecture search for convolutional neural networks. *arXiv preprint arXiv:1711.04528* (2017).
- [14] Alex Fout, Jonathon Byrd, Basir Shariat, and Asa Ben-Hur. 2017. Protein interface prediction using graph convolutional networks. *Advances in neural information processing systems* 30 (2017).
- [15] Yang Gao, Hong Yang, Peng Zhang, Chuan Zhou, and Yue Hu. 2019. Graphnas: Graph neural architecture search with reinforcement learning. *arXiv preprint arXiv:1904.09981* (2019).
- [16] Yang Gao, Hong Yang, Peng Zhang, Chuan Zhou, and Yue Hu. 2021. Graph neural architecture search. In *International joint conference on artificial intelligence*. International Joint Conference on Artificial Intelligence.
- [17] Justin Gilmer, Samuel S Schoenholz, Patrick F Riley, Oriol Vinyals, and George E Dahl. 2017. Neural message passing for quantum chemistry. In *International conference on machine learning*. PMLR, 1263–1272.
- [18] Chaoyu Guan, Ziwei Zhang, Haoyang Li, Heng Chang, Zeyang Zhang, Yijian Qin, Jiyan Jiang, Xin Wang, and Wenwu Zhu. 2021. AutoGL: A Library for Automated Graph Learning. In *ICLR 2021 Workshop on Geometrical and Topological Representation Learning*. <https://openreview.net/forum?id=0yHwpLeInDn>
- [19] Jiayan Guo, Lun Du, Hengyu Liu, Mengyu Zhou, Xinyi He, and Shi Han. 2023. Gpt4graph: Can large language models understand graph structured data? an empirical evaluation and benchmarking. *arXiv preprint arXiv:2305.15066* (2023).
- [20] Qingyan Guo, Rui Wang, Junliang Guo, Bei Li, Kaitao Song, Xu Tan, Guoqing Liu, Jiang Bian, and Yujiu Yang. 2023. Connecting large language models with evolutionary algorithms yields powerful prompt optimizers. *arXiv preprint arXiv:2309.08532* (2023).
- [21] Siyuan Guo, Cheng Deng, Ying Wen, Hechang Chen, Yi Chang, and Jun Wang. 2024. DS-Agent: Automated Data Science by Empowering Large Language Models with Case-Based Reasoning. *arXiv preprint arXiv:2402.17453* (2024).
- [22] Will Hamilton, Zhitao Ying, and Jure Leskovec. 2017. Inductive representation learning on large graphs. *Advances in neural information processing systems* 30 (2017).
- [23] Xiangnan He, Kuan Deng, Xiang Wang, Yan Li, Yongdong Zhang, and Meng Wang. 2020. Lightgcn: Simplifying and powering graph convolution network for recommendation. In *Proceedings of the 43rd International ACM SIGIR conference on research and development in Information Retrieval*. 639–648.
- [24] Xin He, Kaiyong Zhao, and Xiaowen Chu. 2021. AutoML: A survey of the state-of-the-art. *Knowledge-based systems* 212 (2021), 106622.
- [25] Weihua Hu, Matthias Fey, Marinka Zitnik, Yuxiao Dong, Hongyu Ren, Bowen Liu, Michele Catasta, and Jure Leskovec. 2020. Open graph benchmark: Datasets for machine learning on graphs. *Advances in neural information processing systems* 33 (2020), 22118–22133.
- [26] Yuntong Hu, Zheng Zhang, and Liang Zhao. 2023. Beyond Text: A Deep Dive into Large Language Models' Ability on Understanding Graph Data. *arXiv preprint arXiv:2310.04944* (2023).
- [27] Zhao Huan, YAO Quanming, and TU Weiwei. 2021. Search to aggregate neighborhood for graph neural network. In *2021 IEEE 37th International Conference on Data Engineering (ICDE)*. IEEE, 552–563.
- [28] Ganesh Jawahar, Muhammad Abdul-Mageed, Laks VS Lakshmanan, and Dujian Ding. 2023. LLM Performance Predictors are good initializers for Architecture Search. *arXiv preprint arXiv:2310.16712* (2023).
- [29] Shaoxiong Ji, Shirui Pan, Erik Cambria, Pekka Marttinen, and S Yu Philip. 2021. A survey on knowledge graphs: Representation, acquisition, and applications. *IEEE transactions on neural networks and learning systems* 33, 2 (2021), 494–514.
- [30] Maurice G Kendall. 1938. A new measure of rank correlation. *Biometrika* 30, 1-2 (1938), 81–93.
- [31] Thomas N Kipf and Max Welling. 2016. Semi-supervised classification with graph convolutional networks. *arXiv preprint arXiv:1609.02907* (2016).
- [32] Liam Li and Ameet Talwalkar. 2020. Random search and reproducibility for neural architecture search. In *Uncertainty in artificial intelligence*. PMLR, 367–377.
- [33] Shengchao Liu, Weili Nie, Chengpeng Wang, Jiarui Lu, Zhuoran Qiao, Ling Liu, Jian Tang, Chaowei Xiao, and Animashree Anandkumar. 2023. Multi-modal molecule structure–text model for text-based retrieval and editing. *Nature Machine Intelligence* 5, 12 (2023), 1447–1457.
- [34] Microsoft. 2021. Neural Network Intelligence. <https://github.com/microsoft/nni> GitHub repository.
- [35] Christopher Morris, Martin Ritzert, Matthias Fey, William L Hamilton, Jan Eric Lenssen, Gaurav Rattan, and Martin Grohe. 2019. Weisfeiler and leman go neural: Higher-order graph neural networks. In *Proceedings of the AAAI conference on artificial intelligence*, Vol. 33. 4602–4609.
- [36] Babatounde Mochtard Oloulade, Jianliang Gao, Jiamin Chen, Tengfei Lyu, and Raed Al-Sabri. 2021. Graph neural architecture search: A survey. *Tsinghua Science and Technology* 27, 4 (2021), 692–708.
- [37] Adam Paszke, Sam Gross, Francisco Massa, Adam Lerer, James Bradbury, Gregory Chanan, Trevor Killeen, Zeming Lin, Natalia Gimelshein, Luca Antiga, et al. 2019. Pytorch: An imperative style, high-performance deep learning library. *Advances in neural information processing systems* 32 (2019).
- [38] Hongbin Pei, Bingzhe Wei, Kevin Chen-Chuan Chang, Yu Lei, and Bo Yang. 2020. Geom-gcn: Geometric graph convolutional networks. *arXiv preprint arXiv:2002.05287* (2020).
- [39] Hieu Pham, Melody Guan, Barret Zoph, Quoc Le, and Jeff Dean. 2018. Efficient neural architecture search via parameters sharing. In *International conference on machine learning*. PMLR, 4095–4104.
- [40] Yijian Qin, Ziwei Zhang, Xin Wang, Zeyang Zhang, and Wenwu Zhu. 2022. Nas-bench-graph: Benchmarking graph neural architecture search. *Advances in neural information processing systems* 35 (2022), 54–69.
- [41] Esteban Real, Alok Aggarwal, Yanping Huang, and Quoc V Le. 2019. Regularized evolution for image classifier architecture search. In *Proceedings of the aaai conference on artificial intelligence*, Vol. 33. 4780–4789.
- [42] Xubin Ren, Jiabin Tang, Dawei Yin, Nitesh Chawla, and Chao Huang. 2024. A Survey of Large Language Models for Graphs. *arXiv preprint arXiv:2405.08011* (2024).
- [43] Xubin Ren, Wei Wei, Lianghao Xia, Lixin Su, Suqi Cheng, Junfeng Wang, Dawei Yin, and Chao Huang. 2024. Representation learning with large language models for recommendation. In *Proceedings of the ACM on Web Conference 2024*. 3464–3475.
- [44] Alvaro Sanchez-Gonzalez, Jonathan Godwin, Tobias Pfaff, Rex Ying, Jure Leskovec, and Peter Battaglia. 2020. Learning to simulate complex physics with graph networks. In *International conference on machine learning*. PMLR, 8459–8468.
- [45] Prithviraj Sen, Galileo Namata, Mustafa Bilgic, Lise Getoor, Brian Galligher, and Tina Eliassi-Rad. 2008. Collective classification in network data. *AI magazine* 29, 3 (2008), 93–93.
- [46] Olesksandr Shchur, Maximilian Mumme, Aleksandar Bojchevski, and Stephan Günnemann. 2018. Pitfalls of graph neural network evaluation. *arXiv preprint arXiv:1811.05868* (2018).
- [47] Yongliang Shen, Kaitao Song, Xu Tan, Dongsheng Li, Weiming Lu, and Yueting Zhuang. 2024. Hugginggpt: Solving ai tasks with chatgpt and its friends in hugging face. *Advances in Neural Information Processing Systems* 36 (2024).
- [48] Min Shi, Yufei Tang, Xingquan Zhu, Yu Huang, David Wilson, Yuan Zhang, and Jianxun Liu. 2022. Genetic-gnn: Evolutionary architecture search for graph neural networks. *Knowledge-based systems* 247 (2022), 108752.
- [49] Xiangguo Sun, Hong Cheng, Jia Li, Bo Liu, and Jihong Guan. 2023. All in one: Multi-task prompting for graph neural networks. In *Proceedings of the 29th ACM SIGKDD Conference on Knowledge Discovery and Data Mining*. 2120–2131.

- [50] Jiabin Tang, Yuhao Yang, Wei Wei, Lei Shi, Lixin Su, Suqi Cheng, Dawei Yin, and Chao Huang. 2024. Graphgpt: Graph instruction tuning for large language models. In *Proceedings of the 47th International ACM SIGIR Conference on Research and Development in Information Retrieval*. 491–500.
- [51] Yijun Tian, Huan Song, Zichen Wang, Haozhu Wang, Ziqing Hu, Fang Wang, Nitesh V Chawla, and Panpan Xu. 2024. Graph neural prompting with large language models. In *Proceedings of the AAAI Conference on Artificial Intelligence*, Vol. 38. 19080–19088.
- [52] Alexander Tornede, Difan Deng, Theresa Eimer, Joseph Giovanelli, Aditya Mohan, Tim Ruhnke, Sarah Segel, Daphne Theodorakopoulos, Tanja Tornede, Henning Wachsmuth, et al. 2023. Automl in the age of large language models: Current challenges, future opportunities and risks. *arXiv preprint arXiv:2306.08107* (2023).
- [53] Hugo Touvron, Thibaut Lavril, Gautier Izacard, Xavier Martinet, Marie-Anne Lachaux, Timothée Lacroix, Baptiste Rozière, Naman Goyal, Eric Hambro, Faisal Azhar, et al. 2023. Llama: Open and efficient foundation language models. *arXiv preprint arXiv:2302.13971* (2023).
- [54] Petar Veličković, Guillem Cucurull, Arantxa Casanova, Adriana Romero, Pietro Lio, and Yoshua Bengio. 2017. Graph attention networks. *arXiv preprint arXiv:1710.10903* (2017).
- [55] Heng Wang, Shangbin Feng, Tianxing He, Zhaoxuan Tan, Xiaochuang Han, and Yulia Tsvetkov. 2024. Can language models solve graph problems in natural language? *Advances in Neural Information Processing Systems* 36 (2024).
- [56] Haishuai Wang, Yang Gao, Xin Zheng, Peng Zhang, Hongyang Chen, and Jijun Bu. 2023. Graph neural architecture search with gpt-4. *arXiv preprint arXiv:2310.01436* (2023).
- [57] Lei Wang, Chen Ma, Xueyang Feng, Zeyu Zhang, Hao Yang, Jingsen Zhang, Zhiyuan Chen, Jiakai Tang, Xu Chen, Yankai Lin, et al. 2024. A survey on large language model based autonomous agents. *Frontiers of Computer Science* 18, 6 (2024), 186345.
- [58] Xin Wang, Ziwei Zhang, and Wenwu Zhu. 2022. Automated graph machine learning: Approaches, libraries and directions. *arXiv preprint arXiv:2201.01288* (2022).
- [59] Zhili Wang, Shimin Di, and Lei Chen. 2021. Autogel: An automated graph neural network with explicit link information. *Advances in Neural Information Processing Systems* 34 (2021), 24509–24522.
- [60] Zhili Wang, Shimin Di, and Lei Chen. 2023. A Message Passing Neural Network Space for Better Capturing Data-dependent Receptive Fields. In *Proceedings of the 29th ACM SIGKDD Conference on Knowledge Discovery and Data Mining*. 2489–2501.
- [61] Zhenyi Wang, Huan Zhao, and Chuan Shi. 2022. Profiling the design space for graph neural networks based collaborative filtering. In *Proceedings of the Fifteenth ACM International Conference on Web Search and Data Mining*. 1109–1119.
- [62] Lanning Wei, Zhiqiang He, Huan Zhao, and Quanming Yao. 2023. Unleashing the power of graph learning through llm-based autonomous agents. *arXiv preprint arXiv:2309.04565* (2023).
- [63] Lanning Wei, Huan Zhao, and Zhiqiang He. 2022. Designing the topology of graph neural networks: A novel feature fusion perspective. In *Proceedings of the ACM Web Conference 2022*. 1381–1391.
- [64] Lanning Wei, Huan Zhao, Quanming Yao, and Zhiqiang He. 2021. Pooling architecture search for graph classification. In *Proceedings of the 30th ACM International Conference on Information & Knowledge Management*. 2091–2100.
- [65] Wei Wei, Xubin Ren, Jiabin Tang, Qinyong Wang, Lixin Su, Suqi Cheng, Junfeng Wang, Dawei Yin, and Chao Huang. 2024. Llmrec: Large language models with graph augmentation for recommendation. In *Proceedings of the 17th ACM International Conference on Web Search and Data Mining*. 806–815.
- [66] Han Xie, Da Zheng, Jun Ma, Houyu Zhang, Vassilis N Ioannidis, Xiang Song, Qing Ping, Sheng Wang, Carl Yang, Yi Xu, et al. 2023. Graph-aware language model pre-training on a large graph corpus can help multiple graph applications. In *Proceedings of the 29th ACM SIGKDD Conference on Knowledge Discovery and Data Mining*. 5270–5281.
- [67] Keyulu Xu, Weihua Hu, Jure Leskovec, and Stefanie Jegelka. 2018. How powerful are graph neural networks? *arXiv preprint arXiv:1810.00826* (2018).
- [68] Keyulu Xu, Chengtao Li, Yonglong Tian, Tomohiro Sonobe, Ken-ichi Kawarabayashi, and Stefanie Jegelka. 2018. Representation learning on graphs with jumping knowledge networks. In *International conference on machine learning*. PMLR, 5453–5462.
- [69] Chengrun Yang, Xuezhi Wang, Yifeng Lu, Hanxiao Liu, Quoc V Le, Denny Zhou, and Xinyun Chen. 2023. Large language models as optimizers. *arXiv preprint arXiv:2309.03409* (2023).
- [70] Ruosong Ye, Caiqi Zhang, Runhui Wang, Shuyuan Xu, and Yongfeng Zhang. 2023. Natural language is all a graph needs. *arXiv preprint arXiv:2308.07134* (2023).
- [71] Jiaxuan You, Zhitao Ying, and Jure Leskovec. 2020. Design space for graph neural networks. *Advances in Neural Information Processing Systems* 33 (2020), 17009–17021.
- [72] Caiyang Yu, Xianggen Liu, Wentao Feng, Chenwei Tang, and Jiancheng Lv. 2023. GPT-NAS: Evolutionary neural architecture search with the generative pre-trained model. *arXiv preprint arXiv:2305.05351* (2023).
- [73] Hanqing Zeng, Hongkuan Zhou, Ajitesh Srivastava, Rajgopal Kannan, and Viktor Prasanna. 2019. Graphsaint: Graph sampling based inductive learning method. *arXiv preprint arXiv:1907.04931* (2019).
- [74] Lei Zhang, Yuge Zhang, Kan Ren, Dongsheng Li, and Yuqing Yang. 2023. Mlcopilot: Unleashing the power of large language models in solving machine learning tasks. *arXiv preprint arXiv:2304.14979* (2023).
- [75] Muhan Zhang and Yixin Chen. 2018. Link prediction based on graph neural networks. *Advances in neural information processing systems* 31 (2018).
- [76] Shujian Zhang, Chengyue Gong, Lemeng Wu, Xingchao Liu, and Mingyuan Zhou. 2023. Automl-gpt: Automatic machine learning with gpt. *arXiv preprint arXiv:2305.02499* (2023).
- [77] Wentao Zhang, Yu Shen, Zheyu Lin, Yang Li, Xiaosen Li, Wen Ouyang, Yangyu Tao, Zhi Yang, and Bin Cui. 2022. Pasca: A graph neural architecture search system under the scalable paradigm. In *Proceedings of the ACM Web Conference 2022*. 1817–1828.
- [78] Xikun Zhang, Antoine Bosselut, Michihiro Yasunaga, Hongyu Ren, Percy Liang, Christopher D Manning, and Jure Leskovec. 2022. Greaselm: Graph reasoning enhanced language models for question answering. *arXiv preprint arXiv:2201.08860* (2022).
- [79] Mingkai Zheng, Xiu Su, Shan You, Fei Wang, Chen Qian, Chang Xu, and Samuel Albanie. 2023. Can gpt-4 perform neural architecture search? *arXiv preprint arXiv:2304.10970* (2023).
- [80] Kaixiong Zhou, Xiao Huang, Qingquan Song, Rui Chen, and Xia Hu. 2022. Auto-gnn: Neural architecture search of graph neural networks. *Frontiers in big Data* 5 (2022), 1029307.
- [81] Barret Zoph and Quoc V Le. 2016. Neural architecture search with reinforcement learning. *arXiv preprint arXiv:1611.01578* (2016).

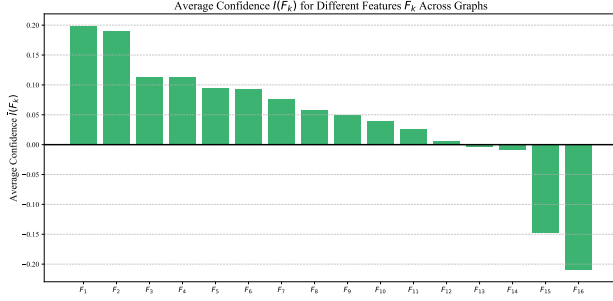


**Figure 6: Average confidence of each graph topological feature across benchmarks.**

## A METHODOLOGY

In this section, we provide a detailed explanation of the methodology behind our DesiGNN framework, including Graph Understanding (Sec. 3.1), Knowledge Retrieval (the settings of accumulated knowledge; Sec. 3.2), and GNN Model Suggestion and Refinement Modules (Sec. 3.3).

### A.1 Algorithm

The DesiGNN methodology is detailed in Algo. 1. The algorithm is divided into three main phases: Graph Understanding, Knowledge Retrieval, and GNN Model Suggestion and Refinement. It also includes details on the Self-evaluation Mechanism, Adaptive Filtering Mechanism, Re-rank Mechanism, Controlled Exploration, Model Promotion Mechanism, and Directional Exploitation and Optimization.

### A.2 Graph Understanding Module

The Graph Understanding Module (Sec. 3.1) is designed to automatically analyze the topological features of graph datasets to enhance task comprehension beyond mere user input. The module initially prioritizes the most influential features based on their influence coefficients averaged across all benchmark datasets, which is illustrated in Fig. 6. The selected features are then used to generate textual descriptions of graph datasets, which are subsequently employed to identify the most similar benchmark datasets for retrieving specialized knowledge.

**A.2.1 Graph Topological Features Pool.** We employ a comprehensive set of 16 graph topological features. The corresponding feature names from  $F_1$  to  $F_{16}$  are listed below (and are also the initialized order based on their confidences  $\bar{I}(F_k)$ ): the average clustering coefficient, average betweenness centrality, density, average degree centrality, average closeness centrality, average degree, edge count, graph diameter, average shortest path length, assortativity, average eigenvector centrality, feature dimensionality, node count, node feature diversity, connected components, and label homophily, to capture the structural characteristics of graph datasets. The underlined features are measured on sampled subgraphs to reduce computational overhead and ensure scalability.

### A.3 Knowledge Retrieval Module

As, the knowledge source of our Knowledge Retrieval Module (Sec. 3.2), NAS-Bench-Graph [40] is a comprehensive benchmark

## Algorithm 1: DesiGNN Methodology

---

**Input:** Unseen Graph Dataset  $G^u$   
**Data:** Benchmark Datasets  $\{G^i\}_{i=1}^n$ ; Benchmark Knowledge Base  $\mathcal{H}_G : \theta \rightarrow P$ ; Task-aware LLMs  $\mathcal{L}\mathcal{L}\mathcal{M}_{GDC}$ ,  $\mathcal{L}\mathcal{L}\mathcal{M}_{IMS}$ ,  $\mathcal{L}\mathcal{L}\mathcal{M}_{MPR}$ ; Adaptive Filter  $\mathcal{F}(\cdot)$ ; Self-evaluation Bank  $BE : \{(G^i, \{F_{ik}\}_{k=1}^6, \{P_{i,j} \mid j \neq i\}_{j=1}^n)\}_{i=1}^n\}$ ; #features  $N_f$ , Knowledge Pool size  $N_s$ , #top models  $N_m$ , #candidates  $N_c$ , stop criteria  $maxTrials$   
**Output:** Optimized GNN architecture  $\theta_u^*$  and model parameters  $\omega^*$

---

```

/* Phase 1: Graph Understanding Module */
1 if  $\mathcal{F}(\cdot)$  needs initialization or update then
    /* Self-evaluation Mechanism */
2   foreach Anchor Dataset  $G^i$  and feature  $F_k \in BE$  do
3     foreach Other Dataset  $\{G^j \in BE \mid G^j \neq G^i\}$  do
4       Compute  $Dist_k^{ij} = \sqrt{(s_{ik} - s_{jk})^2}$  and retrieval
          $P^{ij} \in BE$ 
5     end
6      $SRank(i, k) = \text{argsort}(\{Dist_k^{ij} \mid j \neq i, G^j \in G\}, \text{ascend})$ 
7      $ERank(i) = \text{argsort}(\{P^{ij} \mid j \neq i, G^j \in G\}, \text{descend})$ 
8      $I(G^i, F_k) := \text{KendallCorr}(SRank(i, k), ERank(i))$ 
9   end
    /* Adaptive Filtering Mechanism */
10   $\bar{I}(F_k) = \frac{1}{n} \sum_{i=1}^n I(G^i, F_k)$ 
11  Initialize/Update  $\mathcal{F}(\cdot) = \text{Top}_{N_f}(\{\bar{I}(F_k)\})$ 
12 end
13 Generate unseen dataset's description  $\mathcal{F}(G^u)$  and benchmark
    datasets' descriptions  $\{\mathcal{F}(G^i) \mid G^i \in BE, G^i \neq G^u\}$ 
    /* Phase 2: Knowledge Retrieval Module */
14 Compute  $Sim^u = \{\mathcal{L}\mathcal{L}\mathcal{M}_{GDC}(\mathcal{F}(G^u), \mathcal{F}(G^i))\}_{i=1}^n$ 
15 Retrieve  $KP = \bigcup_{G^i \in \text{Top-}N_s(Sim^u)} \{(G^i, \{\theta_{im}^*\}_{m=1}^{N_m})\}$ 
    /* Phase 3: Initial Model Suggestion */
16 foreach  $KP_i \in KP$  do
17    $\theta_{ui} \leftarrow \mathcal{L}\mathcal{L}\mathcal{M}_{IMS}(\mathcal{F}(G^u), KP_i)$ 
18    $P^{ui} = \mathcal{H}(\theta_{ui}, \omega; G^u)$ 
19 end
20  $BE \leftarrow BE \cup \{(G^u, \{F_{uk}\}, \{P^{ui}\})\}$ 
    /* Phase 4: Model Proposal Refinement */
    /* Re-rank Mechanism */
21  $R = \text{argsort}(\{P^{ui}\}_{i=1}^{N_s}, \text{descend})$ 
22  $KP_{1:N_s} = \{(G^{R[j]}, \{\theta_{R[j]m}^*\}_{m=1}^{N_m})\}_{j=1}^{N_s}$ 
23  $\theta_u^T \leftarrow (\theta_u^{R[1]}, P_u^{R[1]})$ ;  $\theta_u^* = \theta_u^T[1]$ 
24 for  $t = N_s$  to  $maxTrials$  do
    /* Controlled Exploration */
25    $C^t = \{\theta_{ui}^t \mid \text{Crossover}(\theta_u^*, KP_{2:N_s})\}_{i=1}^{N_c}$ 
    /* Model Promotion Mechanism */
26    $\theta_{ui}^t = \text{argsort}(\{\mathcal{H}_{KP_i}(\theta_{ui}^t) \mid \theta_{ui}^t \in C^t\}, \text{descend})[1]$ 
    /* Directional Exploitation and Optimization */
27    $\theta_u^t \leftarrow \mathcal{L}\mathcal{L}\mathcal{M}_{MPR}(\theta_{ui}^t, \theta_u^T, KP_1)$ 
28    $P_u^t = \mathcal{H}(\theta_u^t, \omega; G^u)$ 
29    $\theta_u^T \leftarrow (\theta_u^t, P_u^t)$ 
30   if  $P_u^t > P_u^*$  then
31      $\theta_u^*, \omega^* = \theta_u^t, \omega$ 
32   end
33 end
34 return  $\theta_u^*, \omega^*$ 

```

---

designed to facilitate unified, reproducible, and efficient evaluations of graph neural architecture search (GraphNAS) methods. This benchmark encapsulates a well-defined search space and a rigorous evaluation protocol, which encompasses the training and testing of 26,206 unique graph neural network (GNN) architectures across nine diverse graph datasets.

**A.3.1 Benchmark Datasets.** The benchmark utilizes nine graph datasets of varied sizes and types, including citation networks (Cora, CiteSeer, PubMed) [45], co-authorship graphs (Coauthor CS and Coauthor Physics) [46], co-purchase networks (Amazon Computers and Amazon Photo) [46], and large-scale graphs like ogbn-arXiv [25] from the Open Graph Benchmark. These datasets are employed with fixed semi-supervised [40] splits to ensure consistent evaluation settings.

**A.3.2 Search Space Design.** The search space in NAS-Bench-Graph is constructed as a directed acyclic graph (DAG), representing various GNN architectures. It includes macro architectural choices constrained to 9 distinct patterns:  $[0, 0, 0, 0]$ ,  $[0, 0, 0, 1]$ ,  $[0, 0, 1, 1]$ ,  $[0, 0, 1, 2]$ ,  $[0, 0, 1, 3]$ ,  $[0, 1, 1, 1]$ ,  $[0, 1, 1, 2]$ ,  $[0, 1, 2, 2]$ , and  $[0, 1, 2, 3]$ . The operations include seven prominent GNN layer types—GCN [31], GAT [54], GraphSAGE [22], GIN [67], ChebNet [9], ARMA [2], and k-GNN [35]—plus Identity and fully connected layers for residual connections and non-graph structure use, respectively.

## A.4 GNN Model Suggestion and Refinement

As introduced in Sec. 3.3 and illustrated in Fig. 2, this cycle continues iteratively, with each step methodically enhancing the model architecture based on accumulated knowledge. As illustrated in Fig. 7, the search space is navigated in a controlled manner through simulated crossovers between  $\theta^*$  and configurations from  $KP_{2,s}$ , ensuring that exploration remains within reasonable bounds. Among these generated candidates, the one that demonstrates the highest potential based on its performance on the closest benchmark dataset is identified as the most promising for the unseen dataset. This candidate is then subjected to further strategic refinement by the LLM, guided by the most valuable directional insights derived from  $KP_1$ . Our empirical results support the effectiveness of this approach in quickly refining models. Our retrieval-then-verified promotion strategy not only ensures a reliable and efficient selection of new proposals by leveraging pre-existing, empirically validated knowledge but also requires only a single evaluation per optimization step. This sharply contrasts with more conventional methods that necessitate accumulating knowledge from scratch and running multiple evaluations in parallel, thereby reducing computational overhead and accelerating the refinement process.

## B EXPERIMENTS

### B.1 Experimental Settings

**B.1.1 Task and Data Sets.** We evaluate our DesiGNN framework on eleven diverse graph datasets, including eight out of nine benchmark datasets { Cora [45], Citeseer [45], PubMed [45], CS [46], Physics [46], Photo [46], Computer [46], ogbn-arXiv [25] } from NAS-Bench-Graph [40] and three additional datasets { DBLP [3], Flickr [73], Actor [38] }. All datasets are used to conduct node classification tasks, and their statistics are summarized in Tab. 4. The

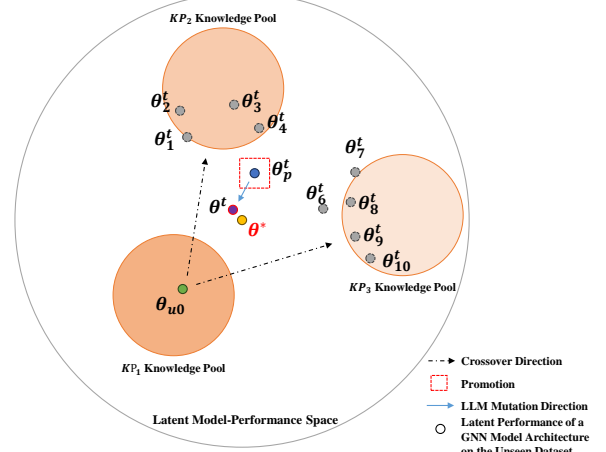


**Figure 7: A conceptual illustration of the controlled exploration and directional exploitation in the GNN Model Suggestion and Refinement.**

**Table 4: The statistic of the datasets**

Dataset	#Vertices	#Links	Features	Classes	Metric
Cora	2,708	5,429	1,433	7	Accuracy
CiteSeer	3,327	4,732	3,703	6	Accuracy
PubMed	19,717	44,338	500	3	Accuracy
CS	18,333	81,894	6,805	15	Accuracy
Physics	34,493	247,962	8,415	5	Accuracy
Photo	7,487	119,043	745	8	Accuracy
Computers	13,381	245,778	767	10	Accuracy
ogbn-arxiv	169,343	1,166,243	128	40	Accuracy
ogbn-proteins	132,534	39,561,252	8	112	ROC-AUC
DBLP	17,716	105,734	1,639	4	Accuracy
Flickr	89,250	899,756	500	7	Accuracy
Actor	7,600	30,019	932	5	Accuracy

reason for excluding ogbn-proteins [25] is that NAS-Bench-Graph only recorded partial model performance due to explosion and out-of-memory errors, making it hard to conduct benchmarking comparisons.

**B.1.2 Training Hyperparameters.** The training hyperparameters used in different datasets are summarized in Tab. 5. For the nine benchmark datasets, we use the same hyperparameters as the NAS-Bench-Graph [40] benchmark to ensure fair comparisons. These hyperparameters were selected based on random searches on 30 anchor GNN architectures. The hyperparameters for the three additional datasets are recommended by LLMs following the same procedure from Graph Understanding (Sec. 3.1) to Initial Model Suggestion (Sec. 3.3.1), except the retrieved knowledge (Sec. 3.2) is replaced by the tuned hyperparameters of the benchmark datasets [40]. All the hyperparameters are fixed across all experiments.

**B.1.3 Module Hyperparameters.** The hyperparameters used in the DesiGNN framework are summarized as follows: the number of topological features  $N_f = 8$  (without semantic description), the size of the knowledge pool  $N_s = 3$  (benchmark datasets with Top-3

**Table 5: Summary of hyperparameters used for each dataset**

Dataset	#Pre-process	#Post-process	Dimension	Dropout	Optimizer	Learning Rate	Weight Decay	Epochs
<b>Cora</b>	0	1	256	0.7	SGD	0.1	0.0005	400
<b>CiteSeer</b>	0	1	256	0.7	SGD	0.2	0.0005	400
<b>PubMed</b>	0	0	128	0.3	SGD	0.2	0.0005	500
<b>CS</b>	1	0	128	0.6	SGD	0.5	0.0005	400
<b>Physics</b>	1	1	256	0.4	SGD	0.01	0	200
<b>Photo</b>	1	0	128	0.7	Adam	0.0002	0.0005	500
<b>Computers</b>	1	1	64	0.1	Adam	0.005	0.0005	500
<b>ogbn-arxiv</b>	0	1	128	0.2	Adam	0.002	0	500
<b>ogbn-proteins</b>	1	1	256	0	Adam	0.01	0.0005	500
<b>DBLP</b>	1	1	256	0.5	SGD	0.1	0.0005	300
<b>Flickr</b>	1	1	128	0.5	Adam	0.001	0.0005	300
<b>Actor</b>	1	1	128	0.5	Adam	0.005	0.0005	400

**Table 6: Best model performance (accuracy with standard derivation) after 10 model validations on the benchmark datasets.**

Type	Model	ACC (STD) %										
		Cora	Citeseer	PubMed	CS	Physics	Photo	Computer	arXiv	DBLP	Flickr	Actor
<b>AutoGL</b>	GNAS	80.89(0.35)	67.45(1.40)	76.36(0.50)	88.94(0.93)	89.55(2.17)	87.76(3.37)	75.70(5.54)	69.84(1.46)	84.67(0.29)	54.69(1.02)	35.12(1.71)
	Auto-GNN	80.63(1.13)	68.45(0.72)	76.35(0.66)	88.46(2.52)	90.94(0.48)	90.08(1.63)	78.39(3.76)	67.78(1.91)	84.84(0.36)	51.27(2.01)	31.32(5.31)
<b>NNI</b>	Random	80.79(0.60)	65.53(4.95)	75.79(0.79)	88.95(1.41)	90.68(0.27)	90.76(1.00)	76.95(3.00)	71.27(0.52)	82.68(5.89)	52.93(1.21)	33.33(3.35)
	EA	81.27(0.59)	67.29(1.37)	74.92(0.88)	88.08(1.61)	91.05(0.64)	89.63(1.26)	80.46(1.88)	70.40(0.50)	85.15(0.33)	54.38(0.87)	33.83(2.65)
	RL	80.28(0.77)	67.39(1.06)	75.39(1.34)	88.47(1.53)	90.70(0.90)	88.84(0.39)	77.48(3.90)	69.12(1.78)	84.46(0.23)	53.34(0.94)	33.61(2.43)
<b>LLMs -based</b>	GPT4GNAS	80.33(0.39)	69.37(0.01)	76.40(0.20)	90.24(0.06)	91.06(0.61)	91.51(0.78)	82.88(1.25)	70.85(0.22)	85.45(0.16)	55.12(0.16)	36.14(0.54)
	GHGNAS	80.51(0.45)	69.30(0.22)	76.49(0.32)	<b>90.28(0.29)</b>	90.94(0.28)	91.64(0.47)	82.40(1.21)	70.88(0.38)	85.42(0.16)	55.00(0.18)	36.56(0.49)
	<b>Our</b>	<b>81.69(0.54)</b>	<b>70.58(0.46)</b>	<b>77.17(0.29)</b>	90.22(0.48)	<b>92.61(0.00)</b>	<b>92.25(0.21)</b>	<b>83.15(0.61)</b>	<b>71.92(0.15)</b>	<b>85.84(0.27)</b>	<b>55.20(0.09)</b>	<b>36.58(2.63)</b>

**Table 7: Performance Ranking of Initial Model Proposals.**

Avg.	Performance Rank (%)								
	Cora	Cit.	Pub.	CS	Phy.	Pho.	Com	arX.	
<b>5.765</b>	5.899	3.324	4.926	11.036	0.053	3.144	7.353	10.383	

similarities to the unseen dataset), the number of top models  $N_m = 30$  (no bad examples), the number of candidates  $N_c = 30$ , and the maximum number of trials  $maxTrials = 30$ . These hyperparameters are selected based on the ablation studies in Sec. C.2, C.3, and C.4, which are fixed across all experiments.

## B.2 Main Results

**B.2.1 Performance Ranking of Initial Model Proposals.** In this section, Tab. 7 presents the performance ranking of initial model proposals within the model space defined by NAS-Bench-Graph [40]. The average performance ranking of initial model proposals across all benchmark datasets is Top-5.77%, indicating that the initial model proposals suggested by our DesiGNN-Init are competitive.

**B.2.2 Model Refinement and Short-run Efficiency.** In this section, we present the complete results of the short-run experiments in Tables 6 (after 10 validations), 8 (after 20 validations), and 9 (after 30 validations). The performance trajectories of all automated baselines are presented in Fig. 8 and 9. The case studies verifying the lack of prior knowledge in LLMs are provided in Tab. 16.

## B.3 Case Studies

**B.3.1 Case Studies: Lack of Prior Knowledge in LLMs.** The first case study verifies the lack of prior knowledge in LLMs about the top-performing models of benchmark datasets within the NAS-Bench-Graph [40] model space (Sec. A.3). The first two columns in Tab. 16 are cases where the semantic description or graph topological features are directly sent to LLMs for model suggestions. The results demonstrate that LLMs are only able to suggest commonly effective layer connections and operations based on user-provided semantic descriptions (left panel) or key graph topological features (middle panel). In fact, we have tested all the benchmark datasets in NAS-Bench-Graph [40] with semantic descriptions, and we found only two macro lists and three operation lists that LLM would recommend regardless of the datasets:

- **Architecture:** [0, 1, 2, 3] and [0, 0, 1, 3].
- **Operations:** ['gcn', 'gat', 'sage', 'skip'], ['gcn', 'gat', 'sage', 'gcn'], and ['gcn', 'gat', 'gin', 'sage'],

After providing the knowledge extracted from our framework to LLMs (right panel), it can be clearly seen that the model it recommends is specialized and has obvious performance improvements.

**B.3.2 Case Studies: Artificial Hallucination in LLMs.** The second case study in Tab. 17 examines the phenomenon of “artificial hallucination” in LLMs when comparing the similarities between the unseen dataset and the benchmark datasets, as detailed in Sec. 3.2.

**Table 8: Best model performance (accuracy with standard derivation) after 20 model validations on the benchmark datasets.**

		ACC (STD) %										
Type	Model	Cora	Citeseer	PubMed	CS	Physics	Photo	Computer	arXiv	DBLP	Flickr	Actor
<b>AutoGL</b>	GNAS	81.35(0.23)	69.49(0.65)	76.94(0.21)	90.12(0.27)	91.64(0.52)	91.47(0.19)	83.15(1.23)	71.49(0.43)	85.51(0.07)	55.22(0.21)	36.82(0.59)
	Auto-GNN	81.07(0.65)	69.78(0.52)	77.21(0.58)	90.36(0.35)	91.92(0.65)	91.52(1.16)	82.73(1.17)	71.50(0.30)	85.65(0.18)	54.99(0.18)	37.10(0.91)
<b>NNI</b>	Random	80.97(0.45)	69.57(0.23)	76.69(0.15)	90.20(0.27)	91.80(0.31)	91.74(0.46)	83.21(0.61)	71.54(0.23)	85.37(0.13)	55.01(0.34)	37.31(0.58)
	EA	81.27(0.59)	67.82(0.93)	76.33(0.70)	89.53(1.03)	91.38(0.51)	91.67(0.49)	82.16(1.17)	71.48(0.27)	85.64(0.25)	55.01(0.23)	36.73(1.48)
	RL	80.53(0.48)	69.69(0.51)	<b>77.33(0.62)</b>	90.30(0.44)	91.48(0.51)	91.75(0.31)	82.46(0.99)	71.22(0.24)	85.44(0.16)	55.01(0.13)	37.52(0.31)
<b>LLMs</b> <b>-based</b>	GPT4GNAS	80.73(0.15)	69.43(0.07)	76.88(0.41)	<b>90.44(0.06)</b>	91.84(0.52)	91.79(0.43)	<b>83.54(0.53)</b>	71.31(0.27)	85.57(0.14)	55.12(0.16)	36.66(0.73)
	GHGNAS	80.66(0.42)	69.44(0.06)	76.93(0.22)	90.42(0.06)	91.59(0.56)	92.03(0.39)	82.93(0.63)	71.44(0.31)	85.43(0.15)	55.06(0.11)	37.01(0.57)
	<b>Our</b>	<b>81.69(0.52)</b>	<b>70.87(0.09)</b>	77.27(0.41)	90.41(0.39)	<b>92.61(0.00)</b>	<b>92.29(0.05)</b>	83.43(0.77)	<b>71.98(0.16)</b>	<b>85.85(0.29)</b>	<b>55.32(0.14)</b>	<b>37.57(0.62)</b>

**Table 9: Best model performance (accuracy with standard derivation) after 30 model validations on the benchmark datasets.**

		ACC (STD) %										
Type	Model	Cora	Citeseer	PubMed	CS	Physics	Photo	Computer	arXiv	DBLP	Flickr	Actor
<b>AutoGL</b>	GNAS	81.35(0.23)	69.67(0.47)	76.97(0.22)	90.18(0.31)	91.92(0.43)	91.61(0.23)	83.23(1.13)	71.54(0.36)	85.58(0.08)	55.23(0.20)	37.23(0.56)
	Auto-GNN	81.46(0.41)	69.78(0.52)	77.37(0.51)	90.50(0.20)	91.92(0.65)	91.97(0.40)	83.06(0.91)	71.61(0.35)	85.66(0.17)	55.20(0.15)	37.50(0.83)
<b>NNI</b>	Random	81.17(0.44)	69.63(0.16)	77.25(0.44)	90.39(0.14)	91.81(0.31)	92.04(0.32)	83.62(0.63)	71.55(0.22)	85.48(0.15)	55.17(0.12)	37.39(0.59)
	EA	81.27(0.59)	68.05(0.70)	76.51(0.83)	89.70(0.80)	91.60(0.65)	91.78(0.60)	83.00(0.84)	71.62(0.26)	85.66(0.24)	55.09(0.21)	37.44(1.86)
	RL	80.91(0.24)	69.88(0.24)	77.33(0.62)	90.47(0.19)	91.83(0.38)	91.75(0.31)	82.48(0.96)	71.47(0.08)	85.52(0.23)	55.05(0.13)	37.52(0.31)
<b>LLMs</b> <b>-based</b>	GPT4GNAS	81.31(0.24)	69.43(0.07)	76.90(0.41)	90.44(0.06)	92.12(0.21)	92.21(0.13)	83.96(0.83)	71.67(0.44)	85.57(0.14)	55.12(0.16)	36.70(0.70)
	GHGNAS	81.39(0.07)	69.64(0.38)	76.93(0.22)	90.42(0.06)	92.06(0.17)	<b>92.38(0.02)</b>	83.28(0.43)	71.84(0.03)	85.47(0.11)	55.06(0.11)	37.01(0.57)
	<b>Our</b>	<b>81.77(0.40)</b>	<b>71.00(0.09)</b>	<b>77.57(0.29)</b>	<b>90.51(0.42)</b>	<b>92.61(0.00)</b>	<b>92.38(0.06)</b>	<b>84.08(0.66)</b>	<b>72.02(0.18)</b>	<b>85.89(0.21)</b>	<b>55.44(0.06)</b>	<b>37.57(0.62)</b>

**Table 10: The ablation study on each component in GNN Model Suggestion and Refinement. \* is our setting.**

		ACC (STD) %							
Method		Cora	CiteSeer	PubMed	CS	Physics	Photo	Computers	arXiv
<b>Initial Proposal Performance</b>									
<b>Feature*</b>		<b>80.31 (0.00)</b>	69.20 (0.16)	<b>76.60 (0.00)</b>	<b>89.64 (0.08)</b>	<b>92.10 (0.00)</b>	<b>91.19 (0.00)</b>	<b>82.20(0.00)</b>	<b>71.50 (0.00)</b>
<b>Semantic</b>		<b>80.31 (0.00)</b>	<b>69.26 (0.00)</b>	75.71 (0.00)	89.53 (0.00)	88.42 (0.00)	91.17 (0.13)	81.79 (1.21)	71.20 (0.34)
<b>Both</b>		<b>80.31 (0.00)</b>	<b>69.26 (0.00)</b>	75.71 (0.00)	89.55 (0.03)	91.45 (0.78)	91.13 (0.07)	<b>82.20(0.00)</b>	<b>71.50 (0.00)</b>
<b>Best Performance After 30 Validations</b>									
<b>All*</b>		<b>81.77 (0.40)</b>	<b>71.00 (0.09)</b>	<b>77.57 (0.29)</b>	<b>90.51 (0.42)</b>	92.61 (0.00)	<b>92.38 (0.06)</b>	<b>84.08 (0.66)</b>	<b>72.02 (0.18)</b>
<b>w/o Re-rank</b>		<b>81.77 (0.40)</b>	69.77 (0.31)	77.40 (0.24)	90.47 (0.00)	92.61 (0.00)	<b>92.38 (0.06)</b>	83.90 (0.14)	71.87 (0.12)
<b>w/o Promotion</b>		81.04 (0.42)	70.33 (0.00)	77.00 (0.30)	90.19 (0.47)	<b>92.71 (0.18)</b>	92.22 (0.16)	82.85 (0.01)	71.99 (0.01)
<b>w/o Exploration</b>		81.61 (0.10)	70.34 (0.64)	77.40 (0.14)	90.24 (0.33)	92.61 (0.00)	91.87 (0.18)	83.74 (0.23)	71.99 (0.08)

Fig. 5 (leftmost) illustrates that the empirically most similar benchmark datasets to PubMed are CS, Physics, and CiteSeer, in descending order of similarity. When employing our Graph Understanding method Sec. 3.1, which leverages key graph topological features (right panel), the top three most similar datasets are CiteSeer, CS, and Physics. However, the current practice that relies solely on semantic descriptions (left panel) identifies Cora, CiteSeer, and ogbn-arxiv as the top three, which does not align with empirical ground truth. This discrepancy arises because LLMs overly rely on the shared characteristic of being citation graphs, assuming that citation datasets like PubMed, Cora, CiteSeer, and ogbn-arxiv should have similar model preferences. This case study demonstrates that relying solely on semantic descriptions is insufficient to capture

the similarities between datasets, which can overwhelm other pertinent information, leading to inaccurate dataset comparisons and ineffective knowledge retrieval.

## C ABLATION STUDIES

To delve deeper into the pivotal designs of DesiGNN, we conducted ablation studies and hyperparameter tunings on three key modules, including Graph Understanding (Sec. 3.1), Knowledge Retrieval (Sec. 3.2), and GNN Model Suggestion and Refinement (Sec. 3.3).

### C.1 Main Ablation Study

We present the main ablation study on the GNN Model Suggestion and Refinement module in Table 10, quantifying the impact of each component in our framework. The results from the initial

**Table 11: Average rankings of different combinations across datasets. A higher rank (with 1 being the highest) corresponds to better performance and lower variability in the initial model proposals.**

Top- $N_s$	Semantic	Combined Rank						
		$g=0$	$g=2$	$g=4$	$g=6$	$g=8$	$g=10$	$g=16$
$N_s=1$	True	2.250	2.312	2.250	2.125	2.437	2.625	2.312
	False	2.562	2.125	2.562	<b>1.812</b>	2.187	2.250	2.125
$N_s=2$	True	2.500	2.187	2.625	1.937	1.687	2.312	2.750
	False	2.625	2.375	2.812	2.000	<b>1.500</b>	2.187	2.250
$N_s=3$	True	2.500	1.937	2.875	1.875	1.937	2.187	2.000
	False	2.125	1.687	2.000	1.750	1.500	<b>1.3750</b>	1.687

**Table 12: The proportion of the best initial model from each dataset in the Top-3 benchmark.**

Scenario	Is Best Initial Model (%)		
	Best	Second	Third
<b>Semantic Only</b>	30.00	50.00	20.00
$N_f = 6$	50.00	22.50	27.50
$N_f = 8$	<b>52.50</b>	<b>37.50</b>	<b>10.00</b>
$N_f = 10$	42.50	40.00	17.50

suggestion stage underscore the importance of designing a proper Graph Understanding method, demonstrating that relying solely on key graph topological features in dataset descriptions outperforms any use of semantic descriptions. In the short-run performance evaluation after 30 model validations, the re-ranking mechanism significantly improves the knowledge-driven model refinement process when the original order of the Knowledge Pool  $KP$  is incorrect. Additionally, the promotion mechanism, which simulates the strategy of human experts refining a model based on accumulated knowledge, plays a crucial role in enhancing the efficacy of model refinement. Lastly, the directional exploration mechanism is empirically beneficial, as it leverages the most relevant model configuration knowledge and the reasoning ability of LLMs to further refine the best candidate model promoted.

## C.2 Ablation Studies on Graph Understanding

In this section, we study the combined effect of the number of selected features  $N_f$  and the usage of semantic description in understanding and comparing graph datasets, under varying sizes  $N_s$  of the Knowledge Pool, which influences the number of initial proposals suggested by LLMs (Sec. 3.3.1). The average rankings of different combinations across datasets in Tab. 11 illustrate that while the optimal  $N_f$  varies with different  $N_s$  values, integrating semantic descriptions often diminishes performance, particularly when  $N_f > 6$  and  $N_s = 3$ . This finding supports our notion of “artificial hallucinations,” where semantic descriptions can hinder the understanding of tasks when sufficient graph topological features are provided.

## C.3 Ablation Studies on GNN Model Suggestion

This study extends from Section C.2 and quantifies the advantage of using the two  $N_s = 2$  or three  $N_s = 3$  most similar benchmarks

**Table 13: Average performance rank of transferring the Top- $N_m$  model designs.**

Top- $N_m$	Average Rank					
	$N_m=1$	$N_m=10$	$N_m=20$	$N_m=30$	$N_m=40$	$N_m=50$
	2.7077	2.8750	2.8438	<b>2.6875</b>	2.9231	2.8769

**Table 14: T-statistic of the ablation studies on the usgae of knowledge-driven Exploration and Re-rank Mechanism with different children number and  $N_s$ .**

Ablation	$N_s$	Children Number=					
		10		20		30	
w/o Re-rank or w/o Exploration							
		True	False	True	False	True	False
w/o Exploration	2	-0.280	0.582	0.512	1.977	0.557	0.566
	3	0.863	0.072	0.055	-0.164	-0.054	-0.358
w/o Re-rank	2	0.647	1.3833	-0.3347	1.2327	-2.0928	-0.8527
	3	-0.1161	-0.8085	-0.5930	-0.5916	-0.7517	-1.9046

**Table 15: Average performance rank of the GNN Model Refinement hyperparameter combinations across benchmark.**

$N_s$	Children Number=	w/o Re-rank					
		10		20		30	
		True	False	True	False	True	False
2	True	7.33	12	7.83	9	13.5	9.17
	False	7.16	14.5	11.7	17.33	16.17	11.83
3	True	11.7	11.17	11.83	9.5	15.33	7.33
	False	12.33	10.17	11.17	10.17	12.83	7

instead of solely the most similar one  $s = 1$ . Tab. 12 calculates the percentage of scenarios where the best initial proposal stems from the first, second, or third most similar benchmark. For  $N_f = 8$  without semantic descriptions, approximately 53% of trials identify the optimal initial proposal from the most similar benchmark, with only 10% benefiting from the third. This data supports a balanced trade-off between performance and efficiency. Notably, this study also serves as the motivation for us to design the Re-rank Mechanism in Model Proposal Refinement (Sec. 3.3.2).

Moreover, we explore the optimal number  $N_m$  of top-performing examples from each benchmark when retrieving the Knowledge Pool and assess the impact of poor examples. Tab. 13 shows that  $N_m = 30$  yields the best average performance across all dataset combinations (2160 records), with further analysis indicating that poor examples do not significantly affect performance outcomes (T-statistic =  $-0.1262$ , P-value =  $0.8998$ ). We thus adopt  $N_m = 30$  without bad examples for an appropriate token length.

## C.4 Ablation Studies on GNN Model Refinement

We investigate the impact of using the  $KP_1$  Knowledge Pool as context for LLMs and the Re-rank Mechanism that is based on initial proposal performance rankings. We also study the best number of children and the effect of adopting different  $N_s$  numbers of knowledge bases to guide the controlled exploration of search space.

Tab. 14 displays T-statistics for various configurations of Knowledge Pool usage and Re-rank Mechanism. For the row of w/o candidate, the True/False columns stand for w/o re-rank, and vice versa. While statistical significance is not reached ( $p\text{-value} > 0.05$ ), certain trends emerge:

- When  $N_s = 3$  knowledge bases are used for a broader perspective, employing a Re-rank Mechanism consistently adds value. This pattern is intuitive as the Re-rank Mechanism will become more influential as the number of knowledge bases increases.
- Broader exploration with  $N_s = 3$  and a larger number of children (e.g., 30) shows that using the  $KP_1$  Knowledge Pool for directed

exploitation is likely effective, as a narrower focus can refine the diversity of potentially immature solutions.

Given the complexity of these patterns, we further assess the performance ranking of GNN Model Refinement hyperparameter combinations across benchmarks to determine the most effective settings. Tab. 15 suggests that the best hyperparameter combination is  $N_s = 3$  and  $N_m = 30$  with both Re-rank Mechanism and  $KP_1$  Knowledge Pool enabled.

Received 20 February 2024; revised 12 March 2024; accepted 5 June 2024



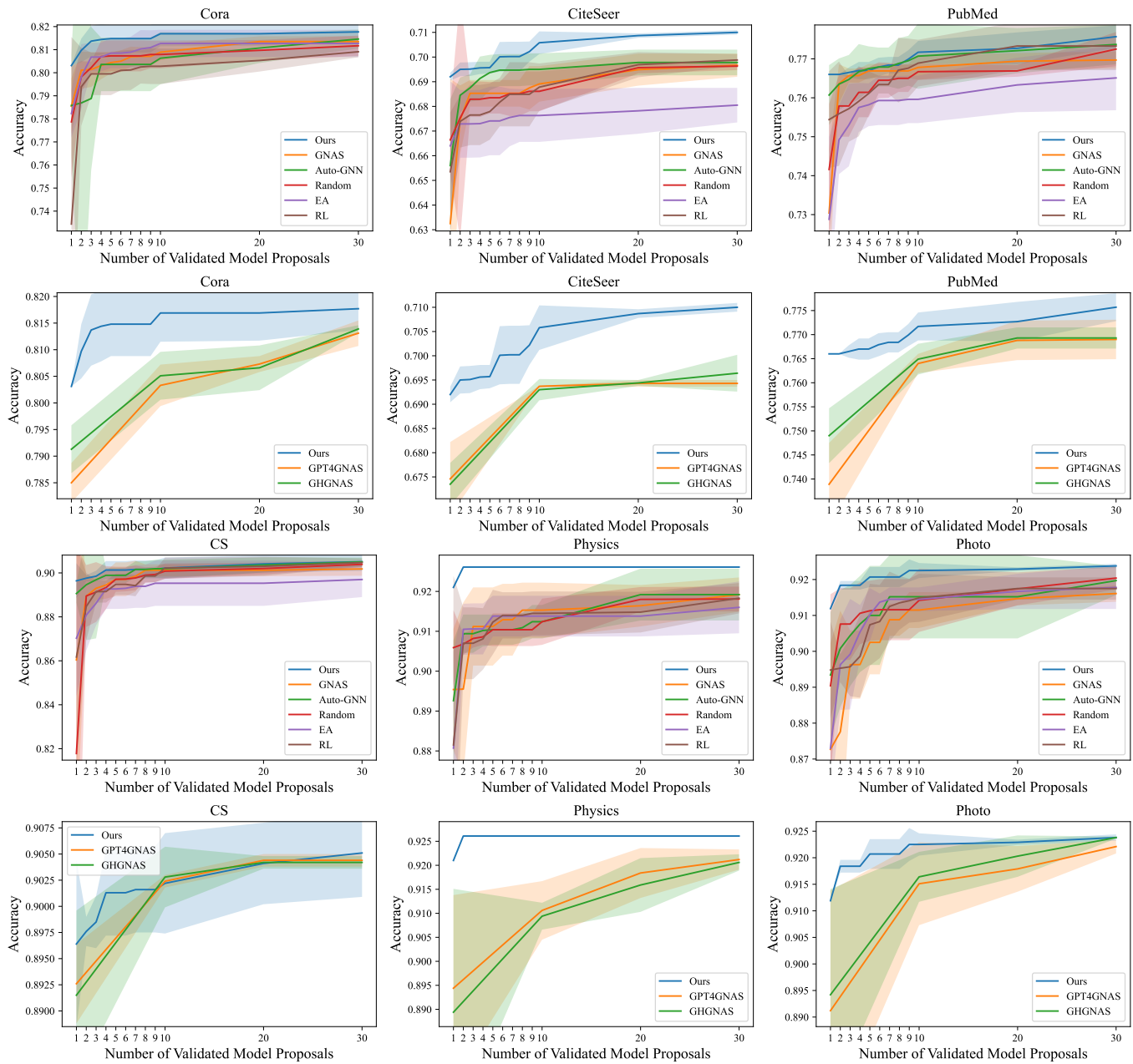


Figure 8: Short-run Performance trajectories of empirically stronger AutoGNN baselines after validating 1, 10, 20, 30 proposals.

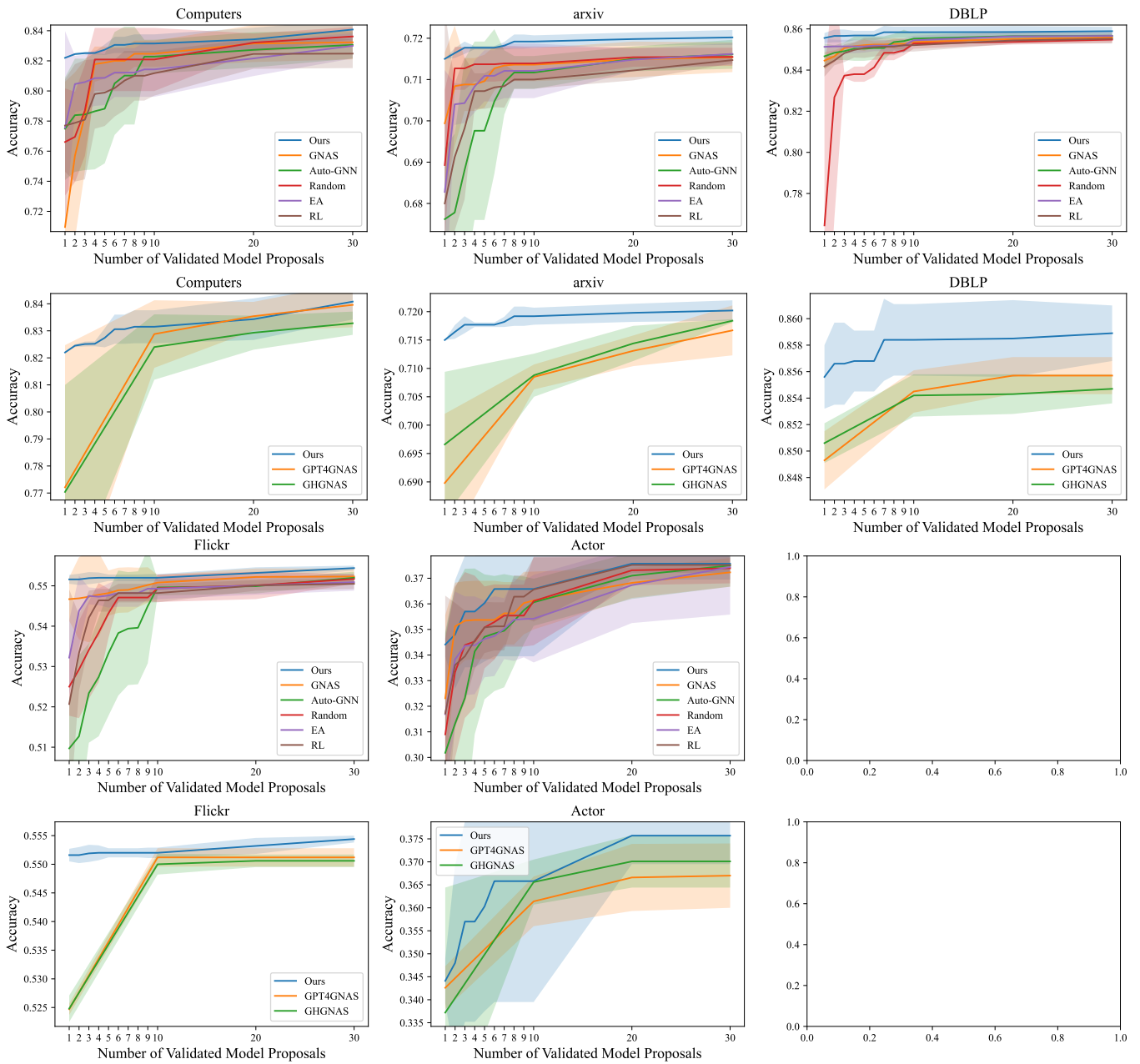


Figure 9: Short-run Performance trajectories of empirically stronger AutoGNN baselines after validating 1, 10, 20, 30 proposals.

**Table 16: Example LLM Response on Recommending Model for PubMed dataset**

Section	Response (w/ Semantic)	Response (w/ Features)	Response (w/ Knowledge)
<b>Decision</b>	For the unseen dataset: (Architecture: [0, 0, 1, 3], Operations: ['gcn', 'gat', 'sage', 'gcn'])	For the unseen dataset: (Architecture: [0, 0, 1, 3], Operations: ['gcn', 'gat', 'sage', 'gin'])	For the unseen dataset: (Architecture: [0, 0, 0, 1], Operations: ['gcn', 'gat', 'arma', 'graph'])
<b>Reason</b>	<p><b>1. Architecture Choice ([0, 0, 1, 3]):</b> This architecture starts with two operations processing the raw input in parallel, followed by a third operation that processes the output of the first operation, and a fourth operation that extends the sequence by processing the output of the third operation. This design allows for both breadth and depth in processing the features:</p> <ul style="list-style-type: none"> <li>- <b>Parallel Processing at the Start:</b> The initial parallel operations allow the model to independently capture different aspects of the input features, which is beneficial for a dataset with a rich feature set like a bag-of-words representation.</li> <li>- <b>Sequential Depth Later:</b> The sequential operations later in the architecture help in refining and integrating the features processed by the earlier layers, which is crucial for capturing the hierarchical structure in citation graphs.</li> </ul> <p><b>2. Operations Choice ([gcn, gat, sage, gcn]):</b></p> <ul style="list-style-type: none"> <li>- <b>First Operation - GCN ('gcn'):</b> The Graph Convolutional Network (GCN) is effective for aggregating neighborhood information, which is essential in a citation graph where the connectivity pattern (citations) plays a crucial role in defining the node (paper) features.</li> <li>- <b>Second Operation - GAT ('gat'):</b> The Graph Attention Network (GAT) introduces an attention mechanism, allowing the model to focus on the most relevant parts of the input graph structure. This is particularly useful in citation graphs for emphasizing influential papers.</li> <li>- <b>Third Operation - GraphSAGE ('sage'):</b> GraphSAGE is adept at sampling and aggregating features from a node's neighborhood, which can help in efficiently handling the local neighborhood structures and diversity in node degrees typical in citation graphs.</li> <li>- <b>Fourth Operation - GCN ('gcn'):</b> Another layer of GCN helps to further refine the feature representation by aggregating higher-order neighborhood information, which can be crucial for capturing the broader context in the graph.</li> </ul> <p>This combination and sequence of operations are designed to leverage both the local and global structural information in the graph, which is critical for a citation graph where both direct and indirect citations (connections) can influence the classification of a paper into topics. The use of both GCN and GAT helps in effectively capturing different levels of granularity in neighbor interactions, while GraphSAGE allows for efficient computation by focusing on a sampled subset of neighbors. The architecture's mix of parallel and sequential processing ensures a comprehensive feature transformation pathway, enhancing the model's ability to learn complex patterns in the data.</p>	<p><b>1. Architecture Choice ([0, 0, 1, 3]):</b></p> <ul style="list-style-type: none"> <li>- The chosen architecture starts with two operations processing the raw input in parallel, followed by a sequential chain. This design allows for initial diverse feature extraction from the raw input, which is crucial given the graph's average degree and density metrics. The sequential steps that follow can refine and enhance the feature representations by integrating information processed in different pathways.</li> <li>- The parallel processing at the beginning ([0, 0]) with 'gcn' and 'gat' allows for both broad and attention-focused neighborhood aggregation. This is particularly useful given the graph's average closeness and betweenness centrality, indicating varying node importance and connectivity.</li> <li>- The subsequent operations ('sage' followed by 'gin') build on the outputs of the initial layers, allowing for further feature enrichment and transformation, which is beneficial given the graph's structural properties like clustering coefficient and diameter.</li> </ul> <p><b>2. Operations Choice ([gcn, gat, sage, gin]):</b></p> <ul style="list-style-type: none"> <li>- <b>'gcn' (Graph Convolutional Network layer):</b> Effective for capturing neighborhood information through a simple yet powerful convolutional approach. Given the average degree and edge count, 'gcn' can efficiently aggregate local neighborhood features without being too computationally expensive.</li> <li>- <b>'gat' (Graph Attention Network layer):</b> Utilizes attention mechanisms to weigh the importance of nodes' neighbors. This is particularly useful in graphs where nodes vary significantly in their roles and influence, as indicated by the centrality measures.</li> <li>- <b>'sage' (GraphSAGE):</b> Samples and aggregates features from a node's neighborhood, which can handle the graph's density and scale effectively. This method is adaptive and can learn from different-sized neighborhoods, which is beneficial given the variability in node connectivity.</li> <li>- <b>'gin' (Graph Isomorphism Network layer):</b> Designed to capture more nuanced graph structural information, which can be crucial for understanding deeper patterns in the graph, especially given the non-trivial graph diameter and clustering coefficient. This combination and sequence of operations are designed to first broadly and then selectively refine the feature representation of the nodes, considering both local and global structural properties of the graph. This should provide a robust model capable of handling the complexities and variabilities in the graph metrics provided.</li> </ul>	<p><b>1. Architecture Choice:</b> The architecture [0, 0, 0, 1] appears frequently among the top-performing models. This configuration starts with three operations processing the raw input in parallel, followed by a fourth operation that processes the output of the first operation. This setup allows for a rich initial feature extraction from the raw input through multiple pathways, followed by a subsequent integration or transformation of these features, potentially capturing complex patterns in the data.</p> <p><b>2. Operation Selection:</b></p> <ul style="list-style-type: none"> <li>- <b>'gcn' (Graph Convolutional Network):</b> This operation is a common choice in many top-performing models. GCN is effective in aggregating neighborhood information, which is crucial for learning representative node embeddings.</li> <li>- <b>'gat' (Graph Attention Network):</b> GAT layers, which utilize attention mechanisms to weigh the importance of nodes' neighbors, are also frequently used. This operation can enhance the model's ability to focus on the most relevant parts of the graph structure.</li> <li>- <b>'arma' (Auto-Regressive Moving Average):</b> ARMA layers have been chosen in various top models, suggesting their utility in capturing more complex dependencies in graph data than standard convolutional layers.</li> <li>- <b>'graph' (k-GNN):</b> The inclusion of a k-GNN operation in the final step can extend the model's capability to capture higher-order interactions, which might be crucial for the specific characteristics of the unseen dataset.</li> </ul> <p><b>3. Combination of Operations:</b> The combination of GCN, GAT, and ARMA before a final GRAPH operation provides a robust sequence of transformations. Starting with GCN allows for a broad capture of neighborhood information, followed by the selective attention mechanism of GAT and the complex filtering of ARMA, culminating in a k-GNN layer that can capture higher-order dependencies. This sequence is designed to progressively refine and enhance the feature representations.</p> <p><b>4. General Observations from Top Models:</b> The selected operations and architecture are among the most recurrent in the top-performing models from similar datasets. This suggests that they are likely to be effective in handling the types of graph-structured data encountered in these benchmarks, making them a prudent choice for the unseen dataset. By synthesizing these observations, the recommended model design aims to balance complexity and depth of feature extraction and transformation, which is crucial for effectively processing graph-structured data. This design is expected to perform well on the unseen dataset by leveraging proven elements from similar successful models.</p>
<b>Performance</b>	75.40	71.56	<b>76.60</b>

**Table 17: Example LLM Response on Dataset Comparison for PubMed dataset**

Benchmark	w/ Semantic Description	w/ Key Graph Topological Features
<b>Cora</b>	<b>Similarity Score: 0.8</b> <b>Reason:</b> Both the unseen dataset and Cora are citation graphs with papers as vertices and citations as links. Both use bag-of-words features and have ground-truth topics as labels. The main differences are in the number of features and classes, with Cora having more features and classes.	<b>Similarity Score: 0.1</b> <b>Reason:</b> The unseen dataset has a significantly higher graph diameter, average closeness centrality, and average betweenness centrality compared to Cora. Additionally, the general graph metrics such as edge count, average degree, and density are quite different, indicating a low similarity.
<b>CiteSeer</b>	<b>Similarity Score: 0.75</b> <b>Reason:</b> Similar to Cora, CiteSeer is also a citation graph with similar characteristics to the unseen dataset. The differences are more pronounced in the number of features and classes, with CiteSeer having significantly more features.	<b>Similarity Score: 0.6</b> <b>Reason:</b> CiteSeer has a closer match in terms of graph diameter and average closeness centrality with the unseen dataset. The average betweenness centrality and general graph metrics like edge count and average degree also show some similarities, suggesting a moderate level of task similarity.
<b>CS</b>	<b>Similarity Score: 0.2</b> <b>Reason:</b> CS is a co-authorship graph, differing significantly in the type of vertices (authors vs. papers) and the nature of features (keywords vs. bag-of-words). The task and evaluation metric are similar, but the structural differences lower the similarity score.	<b>Similarity Score: 0.3</b> <b>Reason:</b> CS shares a similar graph diameter with the unseen dataset but differs significantly in average closeness centrality, average betweenness centrality, and general graph metrics such as edge count and average degree, indicating a moderate to low similarity.
<b>Physics</b>	<b>Similarity Score: 0.2</b> <b>Reason:</b> Similar to CS, Physics is a co-authorship graph with authors as vertices and co-author relationships as links, which is structurally different from the unseen dataset's citation graph nature.	<b>Similarity Score: 0.2</b> <b>Reason:</b> Physics has a similar graph diameter but differs significantly in average closeness centrality, average betweenness centrality, and other general graph metrics like edge count and average degree, suggesting a low similarity.
<b>Photo</b>	<b>Similarity Score: 0.3</b> <b>Reason:</b> Photo is a co-purchase graph, which is different in nature from a citation graph. However, both use bag-of-words features and have a similar number of features, slightly increasing the similarity score.	<b>Similarity Score: 0.1</b> <b>Reason:</b> Photo, while having a similar graph diameter, differs significantly in average closeness centrality, average betweenness centrality, and general graph metrics such as edge count and average degree, indicating a low similarity.
<b>Computers</b>	<b>Similarity Score: 0.3</b> <b>Reason:</b> Similar to Photo, Computers is also a co-purchase graph. The similarity is slightly higher due to a closer number of features and classes compared to the unseen dataset.	<b>Similarity Score: 0.1</b> <b>Reason:</b> Computers has a similar graph diameter but differs significantly in average closeness centrality, average betweenness centrality, and general graph metrics like edge count and average degree, indicating a low similarity.
<b>ogbn-arxiv</b>	<b>Similarity Score: 0.7</b> <b>Reason:</b> ogbn-arxiv is a citation graph similar to the unseen dataset, but it uses word embeddings for features instead of bag-of-words, and has a significantly different number of classes.	<b>Similarity Score: 0.2</b> <b>Reason:</b> ogbn-arxiv shares a similar graph diameter but differs significantly in average closeness centrality, average betweenness centrality, and general graph metrics such as edge count and average degree, suggesting a low similarity.
<b>ogbn-proteins</b>	<b>Similarity Score: -0.5</b> <b>Reason:</b> ogbn-proteins is structurally and fundamentally different from the unseen dataset, being a protein association graph with a multi-label binary classification task and ROC-AUC as the evaluation metric.	<b>Similarity Score: 0.1</b> <b>Reason:</b> ogbn-proteins has a different graph diameter and significantly different average closeness centrality, average betweenness centrality, and general graph metrics such as edge count and average degree, indicating a very low similarity.